NASA TECHNICAL MEMORANDUM

NASA TM-75408

MEASUREMENTS OF TEMPERATURE AND PRESSURE FLUCTUATIONS IN THE T'2 CRYOGENIC WIND TUNNEL

A. Blanchard, J. B. Dor and J. F. Breil

Translation of "Mesures Des Fluctuations De Température Et De Pression Dans La Soufflerie Cryogénique T'2," O.N.E.R.A. Centre d'Etudes et de Recherches de Toulouse, Toulouse, France, OA8/5007 AND (DERAT No. 8.5007 DN) January 1980, 22 pages, 25 diagrams

NATIONAL AERONAUTICS AND SPACE ADMINISTRATION
WASHINGTON, D.C. 20546

OCTOBER 1980

STANDARD TITLE PAGE

1. Report No. NASA TM-75408	2. Government Accession No.	3. Recipient's Catalog No.
4. Title and subtitle MEASUREMENTS OF TEMPERATURE AND PRESSURE FLUCTUATIONS IN THE T'2 CRYOGENIC WIND TUNNEL		5. Report Date October 1980
		6. Performing Organization Code
7. Author(s) A. Blanchard, J. B. Dor and J. F. Briel		8. Performing Organization Report No.
		10. Work Unit No.
9. Performing Organization Name and Address Leo Kanner Associates Redwood City, Calif. 94063		11. Contract or Grant No. NASw-3199
		13. Type of Report and Period Covered Translation
12. Sponsoring Agency Name and Address National Aeronautics and Space Administration, Washington D.C. 20546		14. Sponsoring Agency Code

15. Supplementary Notes

Translation of "Mesures des Fluctuations de Température et de Pression dans la Soufflerie Cryogénique T'2", O.N.E.R.A. Centre d'Etudes et de Recherches de Toulouse, Toulouse, France, OA8/5007 AND (DERAT No. 8/5007 DN) January 1980, 22 pages, 25 diagrams.

16. Abstract Cold wire measurement of temperature fluctuations were made in a DERAT T'2 induction powered cryogenic wind tunnel for 2 types of liquid nitrogen injectors. Thermal turbulence measured in the tranquilization chamber depends to a great extent on the injector used; For fine spray of nitrogen drops, this level of turbulence seemed completely acceptable.

Fluctuations in static pressure taken from the walls of the vein by Kulite sensors showed that there was no increase in aerodynamic noise during cryogenic gusts.

17. Key Words (Selected by Author(s))	18. Distribution Statement
	Unclassified - Unlimited

19. Security Classif. (of this report)	20. Security Classif. (of this page)	21. No. of Pages	22. Price
unclassified	unclassified		

Table of Contents

Annotations

M	The Mach number in the vein
Ti	Temperature when the flow stops
T'	Temperature fluctuation
Pi	Pressure when the flow stops
P'	Static fluctuation
$q = \frac{1}{2} \rho U^2$	Dynamic flow pressure
f	Frequency
$\Delta f = \frac{f_{max}}{128}$	Analysis window
$n = f \cdot \frac{h}{u}$	Reduced frequency, h vein height u speed in the vein
$F_p(n)$	Mean quadratic pressure fluctuations defined by: $\int_0^\infty F_p(n)\, dn = \frac{\overline{P'^2}}{q^2}$

MEASUREMENTS OF TEMPERATURE AND PRESSURE FLUCTUATIONS IN THE T'2 CRYOGENIC WIND TUNNEL

A. Blanchard, J. B. Dor and J. F. Breil
O.N.E.R.A. Centre d'Etudes et de Recherches de Toulouse, Toulouse, France

Introduction

/3*

The difficulties which have occurred in the past few years in correlating transsonic wind tunnel test results with flight tests has led to research into new solutions so we can arrive at Reynolds numbers for wind tunnels akin to those attained in flight tests.

Currently, there are some projects involving cryogenic wind tunnels (the European transsonic high Reynolds number wind tunnel in particular) in which increase in Reynolds numbers is obtained by lowering the flow temperature.

This new concept introduces a new parameter into the use of wind tunnels as the flow temperature may be modified at will. This brings about a certain degree of freedom in the choice of operating conditions (temperature, pressure) when the Mach number and Reynolds number are fixed.

This promising solution does not resolve all the problems. In particular, rigid flow quality conditions were necessary, at the time, for the European transsonic wind tunnel; now, it is difficult to estimate the noise level of any future installation. More generally, we might want to know the flow quality in the crogenic wind tunnel. Atomization and evaporation of the nitrogen produces inevitably fluctuations in temperature. What is the order of magnitude of these fluctuations? At what frequency do they take place? What influence do the measurements have on the results and how might we reduce that

---

* Numbers in the margin indicate pagination in the foreign text.

influence? All these questions should be asked. Moreover, thermal heterogeneity may bring about aerodynamic noise; does this occur in an abnormal fashion in a cryogenic wind tunnel?

/4

To try to resolve these problems, we used a T'2 pilot wind tunnel and a one quarter scale model of a T2 induction powered wind tunnel to measure pressure and temperature fluctuations during a cryogenic gust. We compared these results with those for a gust at ambient temperature. The results of these tests are the subject of this report and are presented after a brief description of the facility, the setup and the procedures used.

1 Description of the Wind Tunnel and Instrumentation

1.1. The T'2 Induction Powered Cryogenic Wind Tunnel

The diagram of the wind tunnel (Fig. 2) shows the circuit with nitrogen injection in the return circuit. A photograph of the facility in dispersed configuration is shown in Fig. 1. The dimensions and principal characteristics of the wind tunnel are given in more detail in the technical report [9].

You will recall that the flow of air-nitrogen gas mixture is started by an injector which delivers two jets of air through the escape edge of the other injector blades on the first turn. In order to compensate for thermal losses as well as the injection of warm air, the liquid nitrogen is vaporized in the return circuit. Since the wind tunnel parameters should remain constant during the gust, we must evacuate the same quantities of air and nitrogen as were injected.

We should also note that the circuit is constructed of ordinary steel. Before it is transformed into a cryogenic wind tunnel, the interior must be insulated. As well as protecting the metal body, this also considerably reduces thermal loss. The interior of the circuit is, therefore, entirely covered with a thin layer of cork three millimeters

in thickness. It is not applied with any particular care to the surface, but is cork sheets readily available on the market. /5

In order to improve flow quality, we tried different ways of injecting the nitrogen which led to a slight modification in the aerodynamic circuit. Injection is no longer done in the return circuit at low speeds but right after the injector bend where the mean flow speed is on the order of Mach 0.6. The first sprayer was therefore redesigned (Fig. 6). We also modified the disposition of the honeycomb and grill work in the plenum chamber (Fig. 6).

1.2. Liquid Nitrogen Injection Systems

Fig. 5 shows a diagram of the nitrogen injection system. Detail and operation were studied during the dynamic liquid nitrogen injection tests described in Technical Report 5/5007 [9].

With the second type of injector described below, the manual control valve and the diagram were removed; the stop valve was located near the injector and connected to the pressurized tank by a 25 mm diameter flexible connector.

1.2.1. Low speed injector

The design of this injector is shown in Fig. 3. It was designed to obtain good spatial temperature homogeneity in the test vein [6].

However, we found, in connection with the ENSAE aerodynamic laboratory [8], that this type of injector generates large drops whose maximum size is about one millimeter because it operates at low nitrogen pressure in a low speed air flow. There are numerous disadvantages /6 to injecting large sized droplets, in particular the length of vaporization time necessary so that the test vein contains no further particles of liquid nitrogen becomes prohibitive.

1.2.2. High speed peripheral injector

In order to obtain the finest possible vapor, we need high pressure in the liquid nitrogen and small diameter injectors. Many injector nozzles must be installed to obtain the necessary output of cooled moving fluid. This injection must take place in a high speed zone, as it is the difference between the flow speed and the speed of the nitrogen particles which blows across the nitrogen jets and accelerates the vaporization of the droplets.

We naturally chose a peripheral injector to reduce load loss to a minimum and we placed it in a high speed zone upstream from the first diffuser (Fig. 4). In this section, whose interior diameter is 119 mm, the mean flow speed is around Mach 0.6; note the presence of two warm moving air jets whose initial speed is Mach 1.6. Mixture of air masses and speed gradients in the first diffuser facilitates the evaporation of the droplets as well as producing uniform temperature. Finally, the injector is placed as far as possible from the test vein. An ENSAE estimate [8] gives, for this case, the maximum size for nitrogen drops in order for complete evaporation to take place in the tranquilization chamber: if we choose an operating temperature of 100 Kelvin at Mach 0.9 and a generating pressure of 2 bars, we find the maximum diameter of the droplets to be 55 microns.

We are currently using the eight nozzle "Fulljet 1/4 HH 6.5" distributed regularly along the perpendicular flow plane, the axis of the jets is situated on this plane; other nitrogen injection nozzles will be tested later. An estimate gives us, in these conditions, a mean diameter of 38 microns for the droplets and a /7 maximum size of 88 microns, both within the acceptable limits.

In order to avoid the false starts which may take place in the injectors at the beginning of the gust due to the bubbles which appear at the contact point of the metal mass which distributes nitrogen to each of the nozzles, a caisson containing liquid nitrogen

was placed around the injector element to ensure cooling prior to the cryogenic gust. An overall view of the unit, installed on the T'2 circuit, is shown in Fig. 7.

1.3. Typical Cryogenic Gust

In order to illustrate the various phases of a cryogenic gust, Fig. 8 shows the pressure, temperature, and Mach number recording.

The wind tunnel is started up at ambient temperature. The pressure rises rapidly to 1.8 bars and the Mach number in the vein soon reaches the fixed value by the second collar section. For our tests we used Mach 0.8. The flow is maintained for about 10 seconds to clean out the wind tunnel at ambient humidity. Then, liquid nitrogen is injected. For 7 or 8 seconds, the gust is established at a temperature chosen beforehand, close to 100°Kelvin for measurement of temperature and dynamics. The pressure rises slightly to 1.9 bars due to the fact that we do not control the evacuation rate.

1.4. Temperature Measurement

The cold wire technique [9] is the technique best adapted to measuring temperature fluctuations. We used a DISA chain operating at a constant current of 0.6 mA in a wire probe whose diameter is 5 microns. Maximum gain (n°11) yields a sensitivity of around 43 mV/Kelvin (the unit does not allow precise sensitivity regulation).

The pass band from a 5 micron cold wire may be estimated at 400 to 500 Hz [7]. /8

1.5. Pressure Measurement

We measured the static pressure on the walls of the vein with a Kulite XCQL sensor placed slightly in back in copper, isolated from the flow by three millimeters of cork to avoid any variation in

temperature of the sensor which might introduce a shift of the zero and variations in sensitivity [9]. Moreover, the risk of thermal gradients and unknown mechanical stresses inside the sensor is thereby eliminated. The cylindrical cavity formed by the positioning of the sensor is very small: 0.6 by 3.5 mm^2. Calculation gives us a natural frequency of 18 kHz. We have shown the importance of cavities upstream of the pressure sensors [1], but we also took several comparative measures at ambient temperatures with a Kulite mounted flush with the wall (Fig. 9). The resonance frequency of the n^o 2 setup was found to be around 8 kHz; this value is only indicative, measurements were used only to give a general indication. Following this we shall limit ourselves to a study of pressure fluctuations at lower frequency: 4 kHz.

We also used a wide pass band (40 kHz) static pressure probe placed outside the boundary layer developing on the vein wall during ambient temperature gusts to show that damage to the surface of the cork and possible alignment errors in static pressure probes did not induce systematic measurement errors.

1.6. Data Acquisition Chain

The T'2 wind tunnel is connected to the T2 acquisition chain [4], made up of a Hewlett-Packard 21 MX computer and a certain number of peripherals shown in Figure 11. The principal peripherals are:

/9

- A digital analog multiplexer-converter,
- a tape drive,
- a disk unit,
- a console with graphic screen,
- a plotting table,
- a printer.

The pressure sensors fed by TEITA-TY 220 datagate deliver output voltage which is boosted by Preston 8300 XWBs. Then, depending on the

case, the signal is either analog-recorded on magnetic tape up to 40 kHz by a Schlumberger Sabre VI, or sent directly to a Rockland filter unit at 48 dB/oct to be digitized at the desired frequency and retained on digital magnetic tape (Fig. 10). Data reduction is done on the spot, immediately after the gust.

1.7. Measurement Reduction

A reduction program was developed on the 21 MX using spectrum calculation of the rapid Fourier transformation, the details of which are given in [3]. Calculation gives the fluctuation energy in a table showing 256 numerical values for 128 lines having a frequency window of $\Delta f = \frac{f_{max}}{128}$; the results of 15 or 20 tables have been averaged.

We did two reductions for each test. One low frequency, 0 to 100 Hz with a sampling frequency of 250 points per second or an analysis window of 0.97 Hz: the other at higher frequencies up to 4 kHz, the sampling frequency being 10,000 points per second giving us a window Δf = 39 Hz.

2 Control of the Technique and Background Noise Measurement

First we verified all measurements of sinusoidal frequencies and those of known regulable amplitude delivered by the signal generator; the results of this reduction should conform to the regulations that we carried out. /10

2.1. Multiplexer Background Noise

Measurements of the digitization noise are obtained by short-circuiting the multiplexer input. There is a resolution of 5 mV and a maximum voltage of 10 volts. Its natural noise, that is to say the aleatory relaxation in the circuit from the 0 level to the 1 level corresponding to 5 mV, is independent of the acquisition rate. We can therefore deduce that the series of figures recorded are always similar.

During reduction, the level of energy found in each one of the lines is reduced to Hertz so as to make the tests directly comparable with each other. We have seen in the case of digitization noise that the energy contained in an analysis band is the same no matter what the acquisition rate is; the result is a Hertz level 40 times weaker than that of an analysis at 4 kHz compared to an analysis done up to 100 Hz.

This can be verified experimentally (Figs. 12, 13, 14 and 15). The digitization noise converted into physical dimensions is obviously a function of the sensitivity of the sensors as we see in Figs. 13 and 15.

We note that the background noise in the filters and amplifiers is lost in the digitization noise. When we short circuit a measurement path upstream of the amplifiers, the noise measured is drowned by the digitization noise.

2.2. Cold Wire Background Noise

While the wind tunnel is at rest, we recorded the signal given out by the cold wire; this represents the natural noise of the probe. /11 A first analysis between 0 and 4 kHz was performed using an analog recorder; it showed a noise level much higher than the digitization noise (Fig. 12): the sensitivity of the probe is 43 mV/Kelvin. By comparison with the spectrum obtained during an ambient temperature gust, we note that significant fluctuations are not measured beyond 700 Hz; we therefore filtered the signal at 1 kHz.

Analysis of the low frequencies made by direct recording reveals the existence of a 50 Hz parasite and its multiples at 100 Hz. We find this noise in the signal delivered by the cold wire during an ambient temperature gust (Fig. 13).

2.3. Pressure Sensor Background Noise

The sensitivity of a static pressure sensor used during the tests

is 8.44 volt/bars.

For an analysis up to 4 kHz, the background noise of Kulite, determined from analog recording taken while the wind tunnel is at rest, is clearly different from the digitization noise (Fig. 14). It is not the same as in the analysis of the low frequencies in which this level is about equal with the multiplexer noise (Fig. 15). Note that the analog recorder is used only to determine spectrum differences at high frequencies; this explains the difference we found in the energy levels at low frequencies (Figs. 14 and 15).

Similarly to the cold wire, there is a perturbation in the signal at 50 Hz, but this is less important for measurement of fluctuations in pressure recorded in the test vein during an ambient temperature gust (Fig. 15). The voltage amplifier used added a parasitic frequency around 400 Hz (Fig. 14). We did not believe that this defect had a negative influence on the good quality of our measurements.

3 Presentation of Results /12

3.1. Wind Tunnel Noise at Ambient Temperature

Prior studies on flow quality in an induction powered transsonic wind tunnel were done on T'2 and T2, in order to compare LEHRT European Pilot Project wind tunnel performances [2].

The relation of the mean noise level to the dynamic pressure q of the ambient temperature flow was compared to tne level found beforehand in the T'2 wind tunnel (Fig. 16). For a Mach number of 0.8 and a second startup collar, we obtained a relative fluctuation of 3.9% during a spectral analysis up to 4 kHz. This level is slightly higher than that obtained previously, a result which was entirely predictable given the modifications done to the circuit, and in particular, the installation of the internal covering whose surface state and junctions were of mediocre quality, especially in the most

delicate parts, that is the elbows and their blades.

It is also interesting to compare our results to spectra measured in the T2, thus bringing out the contribution of low frequencies and boundary level noise [2]. This spectrum is presented in a standardized form (Fig. 17) in which n is a quantity such that

$n = f \cdot \frac{h}{u}$ with:

- f = the frequency in Hertz,
- h = the height of the experimental vein in meters,
- u = the flow speed in m/s.

We carry this quantity in ordinates without dimension $\sqrt{n\ F_p(n)}$ in which $F_p(n)$ represents the mean quadratic fluctuation in pressure defined by:

$$\int_0^\infty F_p(n)\, dn = \overline{P^2}/q^2$$

At low frequencies we find the same level of fluctuation found in the T2 under similar conditions, nozzle ratio $\lambda = 20$ and the second throat which largely attenuates the low frequencies by making it harder for the natural noise of the nozzle to return to the test vein. /13

On the other hand, the boundary layer noise which corresponds to the part of the spectrum in which n is greater than 0.1 is noticeably higher. In order to verify that the displacement is not induced by poor quality pressure probes on the wall, we took a measurement in the center of the flow using a static pressure probe whose membrane cavity had been reduced to a minimum. The result obtained (Fig. 18) confirmed the spectrum measured beforehand; this would seem to indicate that the natural noise of the boundary layer is greater in the circuit because of the rough wall surface.

3.2. Temperature Fluctuations in the Cryogenic Flow

We analyzed the signal from 40 Hz to 1 kHz, delivered by the cold

wire during a cryogenic gust stabilized at a temperature of around 105 Kelvin, 1.9 bars of pressure, and Mach 0.8.

The spectrum obtained with the new nitrogen injector, which produced a finer vaporization, is compared to the spectrum measured during an ambient temperature gust. (Fig. 19). The mean quadratic level of fluctuation is 0.19 Kelvin (0.13 Kelvin for a classic gust), the two spectra are very close.

On the other hand, spectral analysis of low frequencies (from 1 Hz to 100 Hz) reveal a larger divergence (Fig. 20). The mean quadratic fluctuations are 0.27 Kelvin in the cryogenic state as compared with 0.20 Kelvin for an ambient temperature gust. These figures seem abnormal compared with the preceding ones. In fact, it is the low frequencies which possess the maximum energy. By eliminating the first line showing continuous voltage, during a /14 high frequency analysis, we also eliminate the frequency band with the highest energy fluctuation.

These mean quadratic values present another anomaly; the divergence observed on the spectra (Fig. 20) indicates that there is a wider divergence in fluctuation. A look at the tracings produced during ambient temperature flow clearly shows a parasitic frequency at 50 Hz that does not exist during a cryogenic gust. This is due to the fact that the ratio of signal to noise is almost ten times greater. It is appropriate, therefore, to eliminate this peak when calculating the mean quadratic value which is finally found to be 0.08 Kelvin.

We also analyzed the thermal turbulence of the flow in the tranquilization chamber while nitrogen injection was taking place in the return circuit with the old injector. We compared the results obtained with the two types of injection (Fig. 21). The turbulence is considerably higher, the mean quadratic fluctuation is 1.16 Kelvin as compared to the preceding figure of 0.27 Kelvin.

It is altogether probable that in the old configuration there were a large number of liquid nitrogen droplets which had not completely

evaporated before reaching the tranquilization chamber. The impact of these droplets is not great enough to disturb the spectral analyses at the frequencies studied as the two curves seem to be mildly divergent.

Note also that the spectra obtained during a cryogenic flow are altogether similar to those taken from a wind tunnel functioning at ambient temperatures; only the energy level is higher.

3.3. Static Pressure Fluctuations During Cryogenic Flow

The spectra presented here were measured at the wall with a Kulite sensor whose gauges were shown not to deviate. /15

A primary frequency analysis at 40 Hz to 4 kHz revealed no significant divergence between ambient temperature flow and flow cooled by a fine nitrogen vapor (Fig. 22); a slight divergence can be seen but only at frequencies greater than 800 Hz. The mean quadratic value of the fluctuations in static pressure brought back to the dynamic flow pressure q is 3.9% at ambient temperature and 4.6% for the cryogenic state.

A study of the low frequencies (Fig. 23) does not show any modifications in the pressure fluctuation spectra. The mean quadratics for fluctuations measured up to 100 Hz are 2.6% and 2.57%; these values are obviously lower than those obtained from analysis at 4 kHz.

We also compared the spectra obtained during cryogenic flow with two types of nitrogen injectors (Fig. 24). We see that they are altogether similar; injection in the return circuit yields the same level, although slightly weaker, 2.10% as opposed to 2.57%, fluctuation. This is ample confirmation for the results obtained, taking the elevated level of thermal turbulence into account.

3.4. Wind Tunnel Noise During Cryogenic Gusts

The fluctuation spectra for static pressure may be presented in a standardized form as in paragraph 3.1. At equal frequency and fixed

Mach number in the test veins, the value $n = f.h/u$ varies as $(T)^{-1/2}$ in which T is the flow temperature; for a cryogenic gust at a temperature of 105 Kelvin, this number is multiplied by 1.62.

We showed (Fig. 25) the standardized spectra obtained during both ambient temperature and cryogenic flow. It is evident from the curve that, apart from a slight deviation seen in frequencies higher than 800 Hz (Fig. 22) which is compensated in part by slippage /16 in the lower frequencies, the two spectra may be superimposed. There is, therefore, no boundary layer noise modification.

In the tables below we give the mean quadratic fluctuation values measured during various spectral analyses.

TEMPERATURE FLUCTUATIONS $\sqrt{\overline{T_i'^2}}$

		Analysis at 1...100 Hz	Analysis at 40...1000 Hz
Ambient temperature (M = 0.8 (P_i = 1.8 bars (T_i = 275 Kelvin		corrected value at 0.08 Kelvin	corrected value at 0.07 Kelvin
Cryogenic temperature	Peripheral LN2 injector 1st diffuser	0.27 Kelvin	0.19 Kelvin
(M = 0.8 (P_i = 1.9 bars (T_i = 105 Kelvin	Return circuit LN2 injection	1.16 Kelvin	

RELATIVE PRESSURE FLUCTUATIONS $\sqrt{\overline{P'^2}} / q$

		Analysis 1...100 Hz	Analysis 40...4000 Hz
Ambient temperature		2.6%	3.9%
Cryogenic temperature	LN2 Injection 1st diffuser	2.57%	4.6%
	Return circuit LN2 injection	2.10%	

Conclusion

The experiments conducted in the T2 transsonic wind tunnel /17
clearly show the influence of injection of liquid nitrogen on thermal turbulence measured in the tranquilization chamber. Temperature fluctuations were not measured in the test vein during this study because we used the cold wire technique. The rapid response of the thermocouple, however, during experiments conducted at much lower Mach numbers using the cold wire showed us that the thermal turbulence in the test vein was identical to that measured in the tranquilization chamber. Generally speaking, the convergence did not seem to have beneficial effects on the temperature gradients and fluctuations.

Nevertheless, the thermal turbulence resulting from a peripheral injection in a high speed circuit seems to have a completely acceptable level, and we can reasonably suppose that this parameter will not have a detrimental influence on the quality of the measurements taken in a cryogenic wind tunnel of this type.

The temperature spectra measured in a flow cooled by liquid nitrogen do not differ from the spectra measured at ambient temperature save the difference of the energy level of their fluctuations. We may consider thermal turbulence to be found essentially in the very

low frequencies.

Temperature fluctuations measured under the most unfavorable conditions have little influence on the fluctuation in static pressure measured in the test vein; especially in the low frequencies where such modifications might have been expected. During cryogenic operations, wind tunnel noise is therefore identical to noise natural to the facility.

We found a natural boundary layer noise higher than that found in the T2 wind tunnel operating under similar conditions; this increase /18 being due to the various modifications made to the aerodynamic circuit and especially to the poor quality of the wall surface.

The object of the experiment which lead us to these divergent results was to find solutions to the problems of thermal and dynamic noise in cryogenic gust wind tunnels. We could imagine many other procedures which would reduce this noise to a level close to that at which ambient temperature wind tunnels operate, but, for the present, these results seem altogether satisfactory.

References

1. Quemard, C., Mignosi, A., and Seraudie, A., Technical Report "Studies in the induction powered pressurized transonic wind tunnel. Qualities of flow in the T'2 pilot installation," (DERAT) No. 11/5006 DN, May, 1976. /19

2. Mignosi, A., Seraudie, A, and Planazet, M, Technical Report "Measurement of the fluctuations in flow in T'2 and T2 induction powered transonic pilot wind tunnels," (DERAT) No. 2/5007 DN, January, 1977.

3. Gobert, J.L., Technical Report "A method for analyzing fluctuations in flow in a wind tunnel using a minicomputer," (DERAT) No. 1/0057 DN, October, 1976.

4. Gobert, J.L., Technical Report "Acquisition means used for the DERAT T2 wind tunnel," (DERAT) No. 22/5006 DN, September, 1979.

5. Michel, R., and Faulmann, D., "Preliminary tests in a cryogenic transonic wind tunnel driven by induction," Spring meeting of Supersonic Tunnel Association, El Segundo, California, USA, April 17-18, 1978. T. P. ONERA No. 1978-48E

6. Blanchard, A., and Faulmann, D., "Progress report on a cryogenic transonic wind tunnel driven by induction," Symposium on Cryogenic Wind Tunnels, Paper 13, Southampton (G.B.), April 3-5. 1979.

7. Liousse,F., Calvet, P,, and Giovannini, A., "Experimental study of thermoresistive sensors under cryogenic conditions," Symposium on Cryogenic Wind Tunnels, Paper 4, Southampton (G.B.), April 3-5, 1979. /20

8. Luneau,J., Rochas, N., and Kirmann, C., "Preliminary study of the injection process of LN2 in a cryogenic wind tunnel," Symposium on Cryogenic Wind Tunnels, Paper 14, Southampton (G.B.) April 3-5, 1979.

9. Blanchard, A., and Dor, J.B., The Final Minutes CA No. 5/5007 AYD, "Dynamic tests done on the T'2 cyrogenic wind tunnel resulting from a variation in the injection of liquid nitrogen," (DERAT No. 5/5007 DY) April, 1979.

List of Figures /21

Fig. 14: Noise from the pressure sensors at high frequencies (4 kHz). /22

Fig. 15: Noise from the pressure sensors at low frequencies (100 Hz).

Fig. 16: Mean level of fluctuation in static pressure measured in the T'2 wind tunnel.

Fig. 17: Normalized spectrum of static pressure fluctuations.

Fig. 18: Comparison of the spectra taken from the wall and the flow center.

Fig. 19: Temperature fluctuation spretrum taken during a cryogencic flow up to 1 kHz.

Fig. 20: Temperature fluctuation spectrum taken during a cryogenic flow up to 100 Hz.

Fig. 21: Comparison of temperature spectra obtained with two types of liquid nitrogen injectors.

Fig. 22: Pressure fluctuation spectrum taken during cryogenic flow up to 4 kHz.

Fig. 23: Pressure fluctuations taken during cryogenic flow up to 100 Hz.

Fig. 24: Comparison of pressure spectra obtained with two types of liquid nitrogen injectors.

Fig. 25: Comparison of wind tunnel noise at ambient temperature and during cryogenic flow.

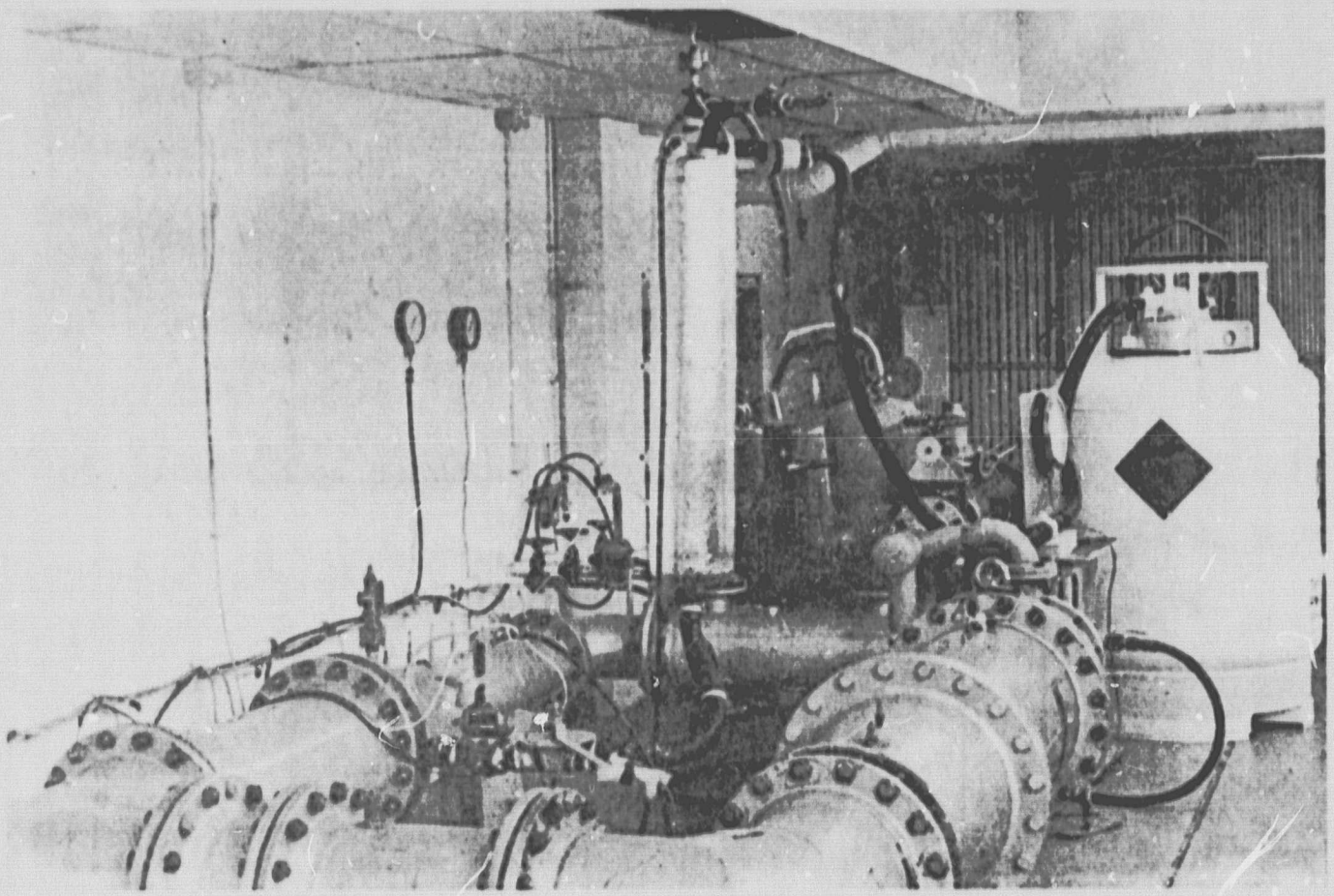

Figure 1: An overall view of the T'2 wind tunnel and its liquid nitrogen injection system.

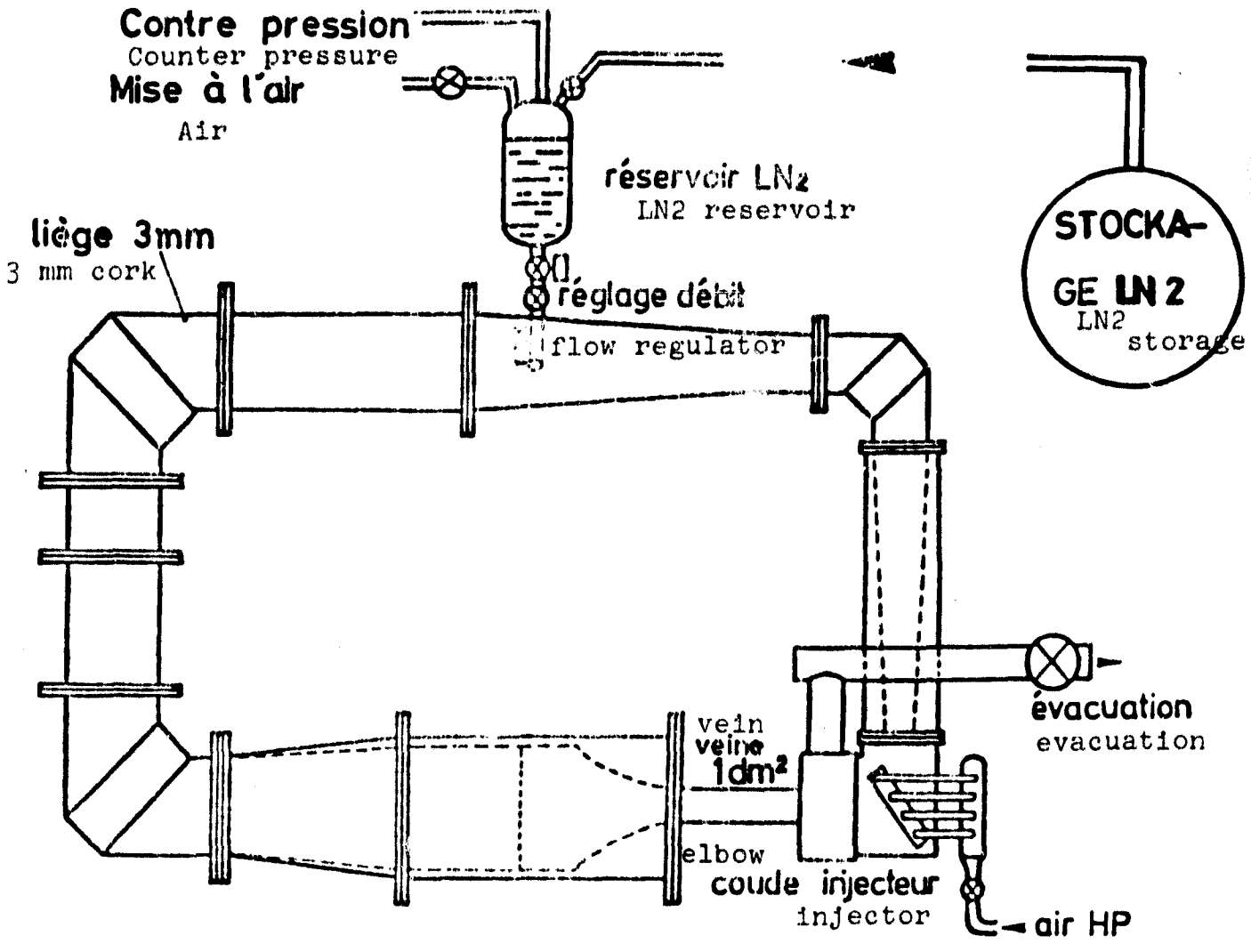

Figure 2: A diagram of the wind tunnel with nitrogen injection in the return circuit.

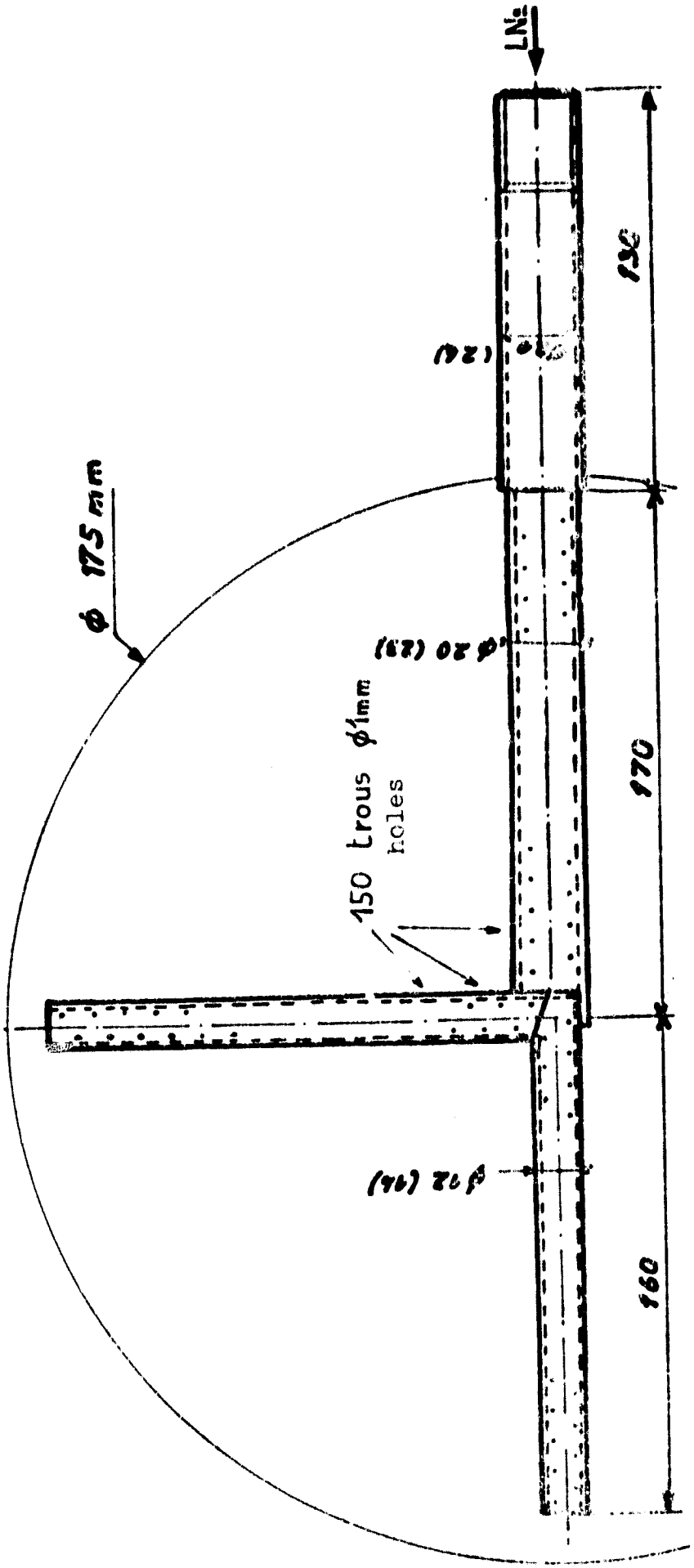

Figure 3: Liquid nitrogen injector of the first type in the return circuit.

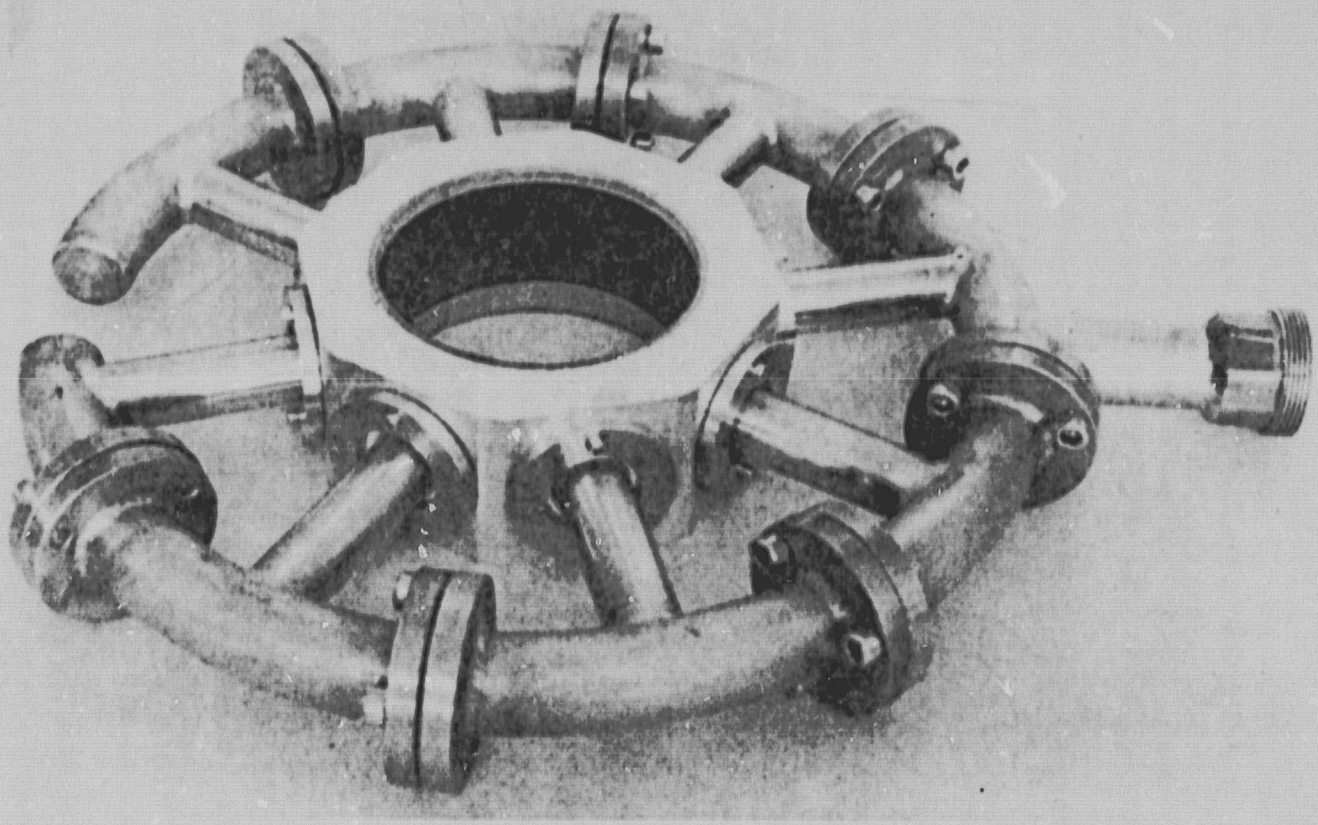

Figure 4: Peripheral injector for liquid nitrogen in the high speed circuit.

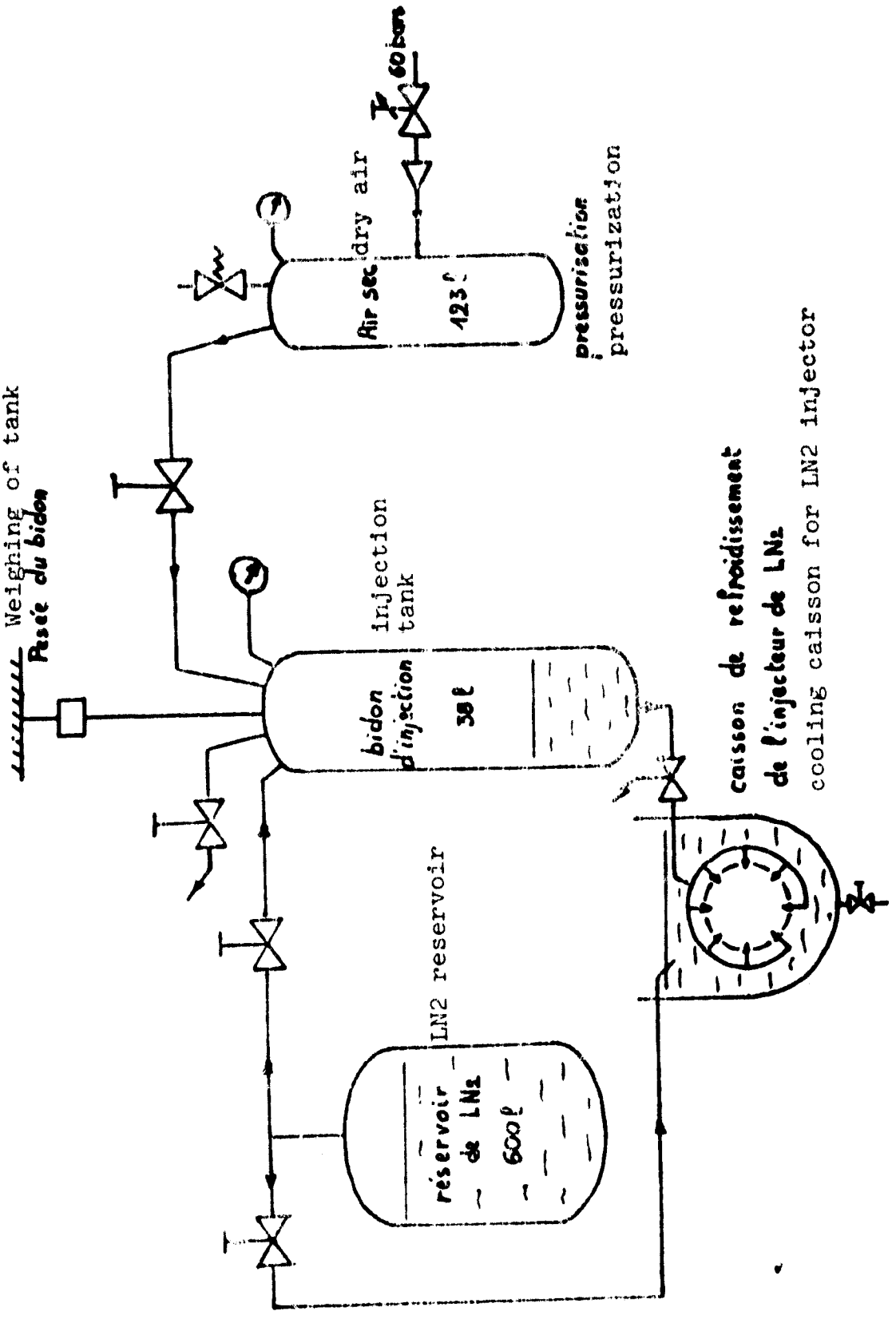

Figure 5: Liquid nitrogen injection system.

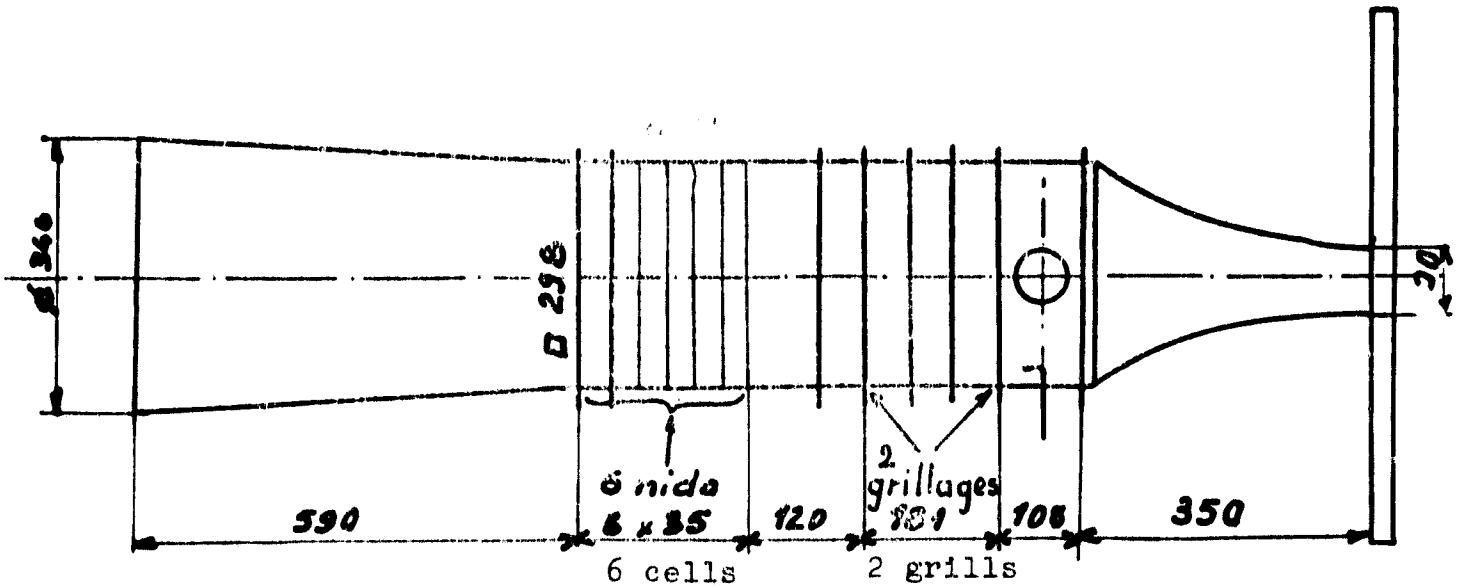

Chambre de tranquilisation_Collecteur

Plenum chamber-collector

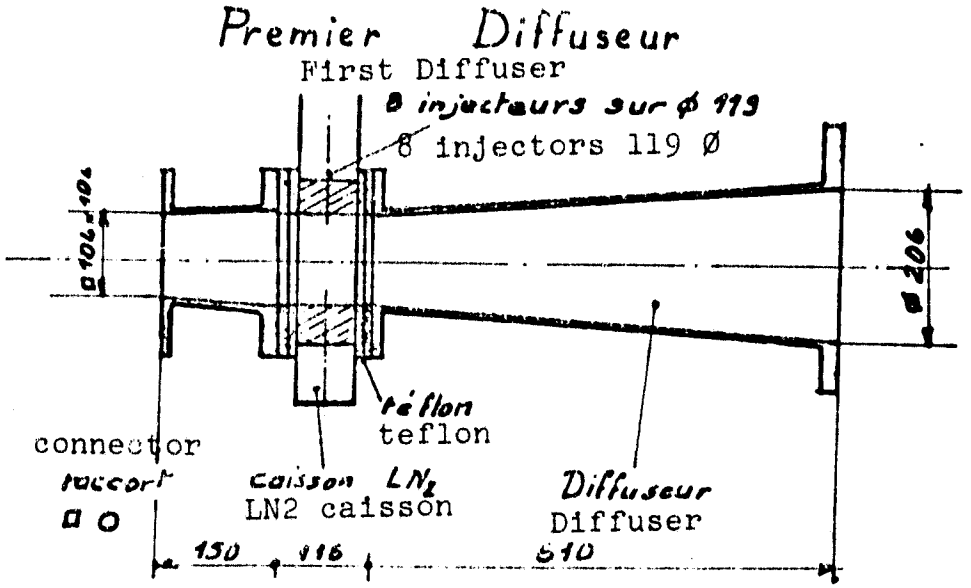

Figure 6: Modifications on the T'2 circuit for the installation of the peripheral injector.

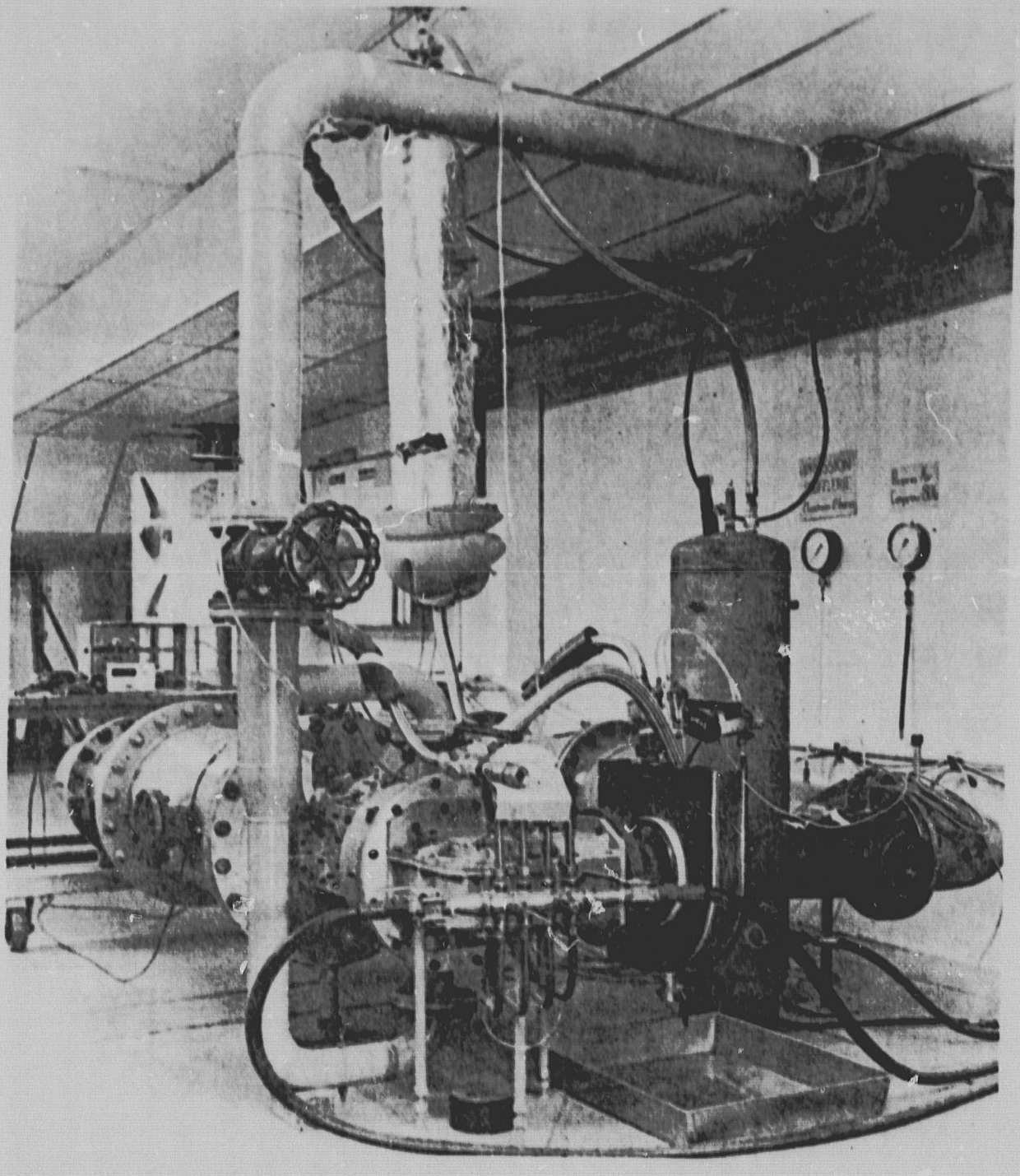

Figure 7: LN2 injector and its cooling caisson installed in the first diffuser.

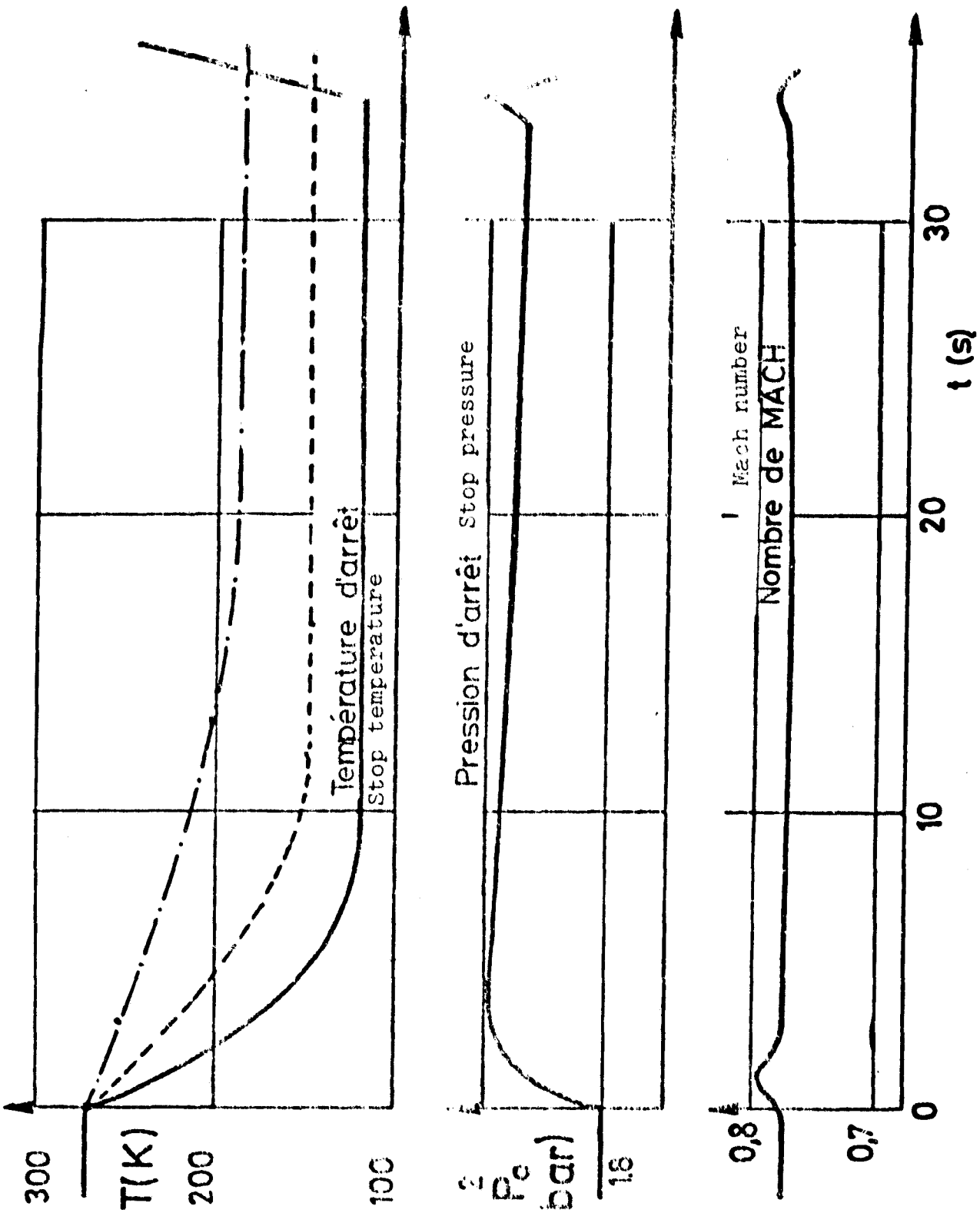

Figure 8: Typical cryogenic gust.

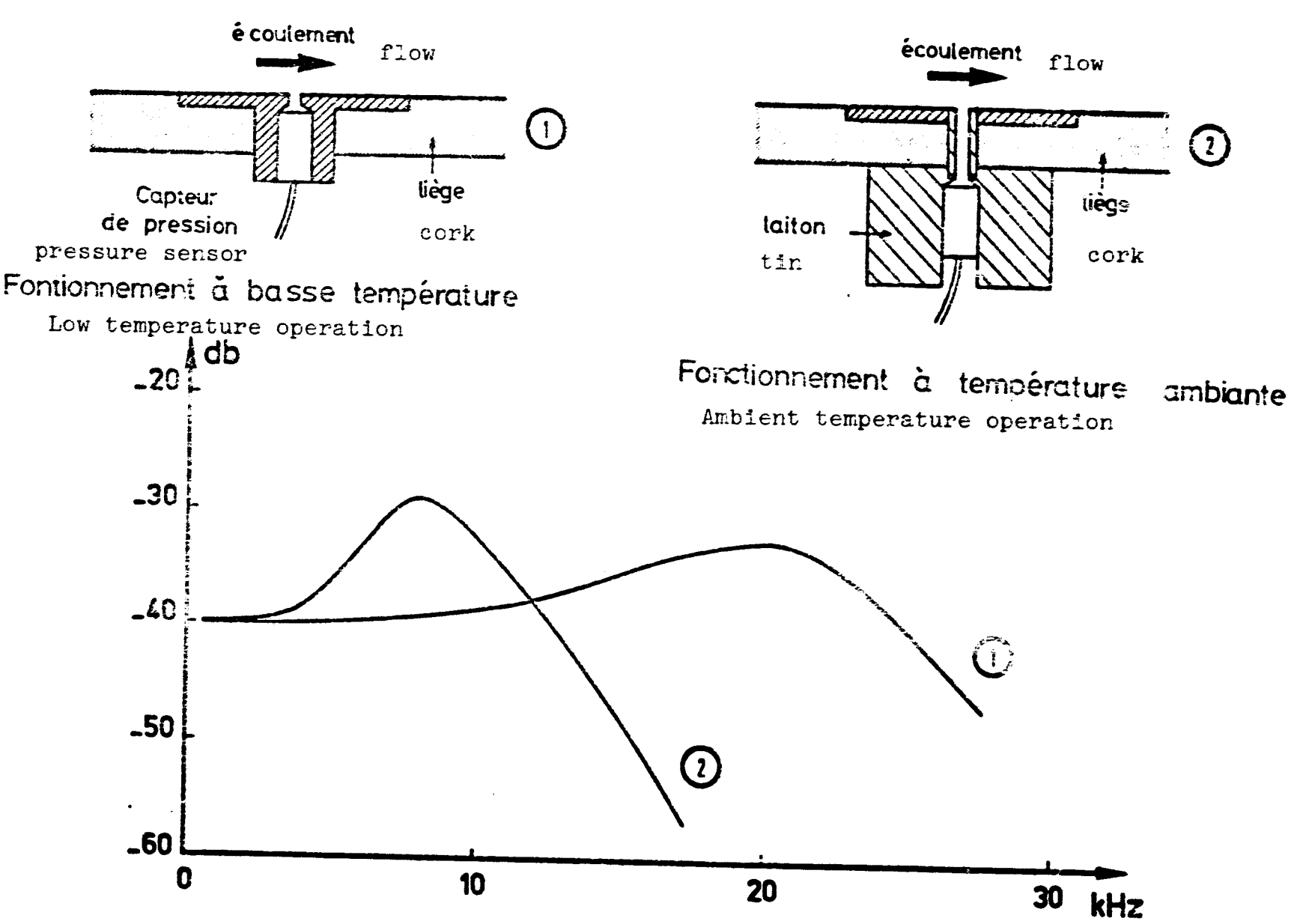

Figure 9: Comparison of the pass band of Kulite sensors in the two different wall setups.

PL. 9

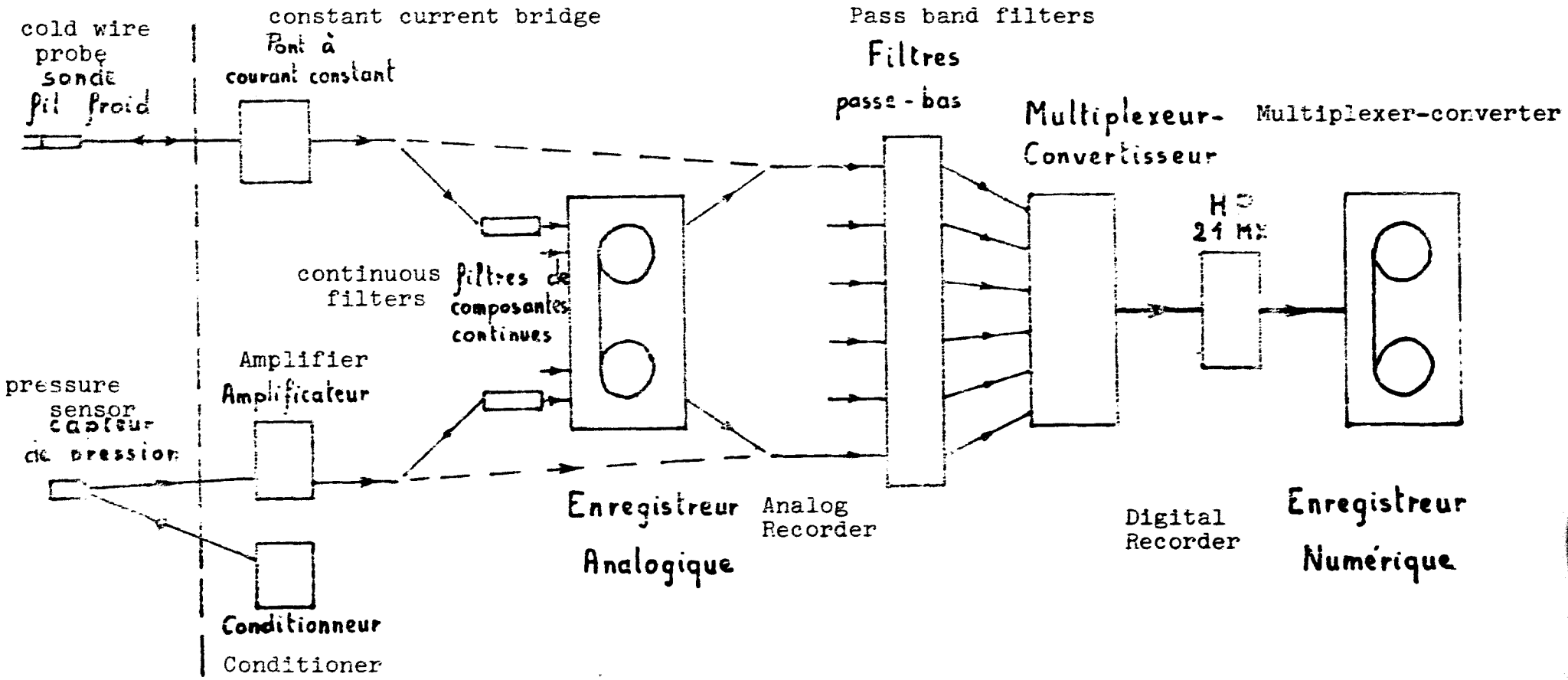

Figure 10: Diagram of the measurement chain.

PL. 10

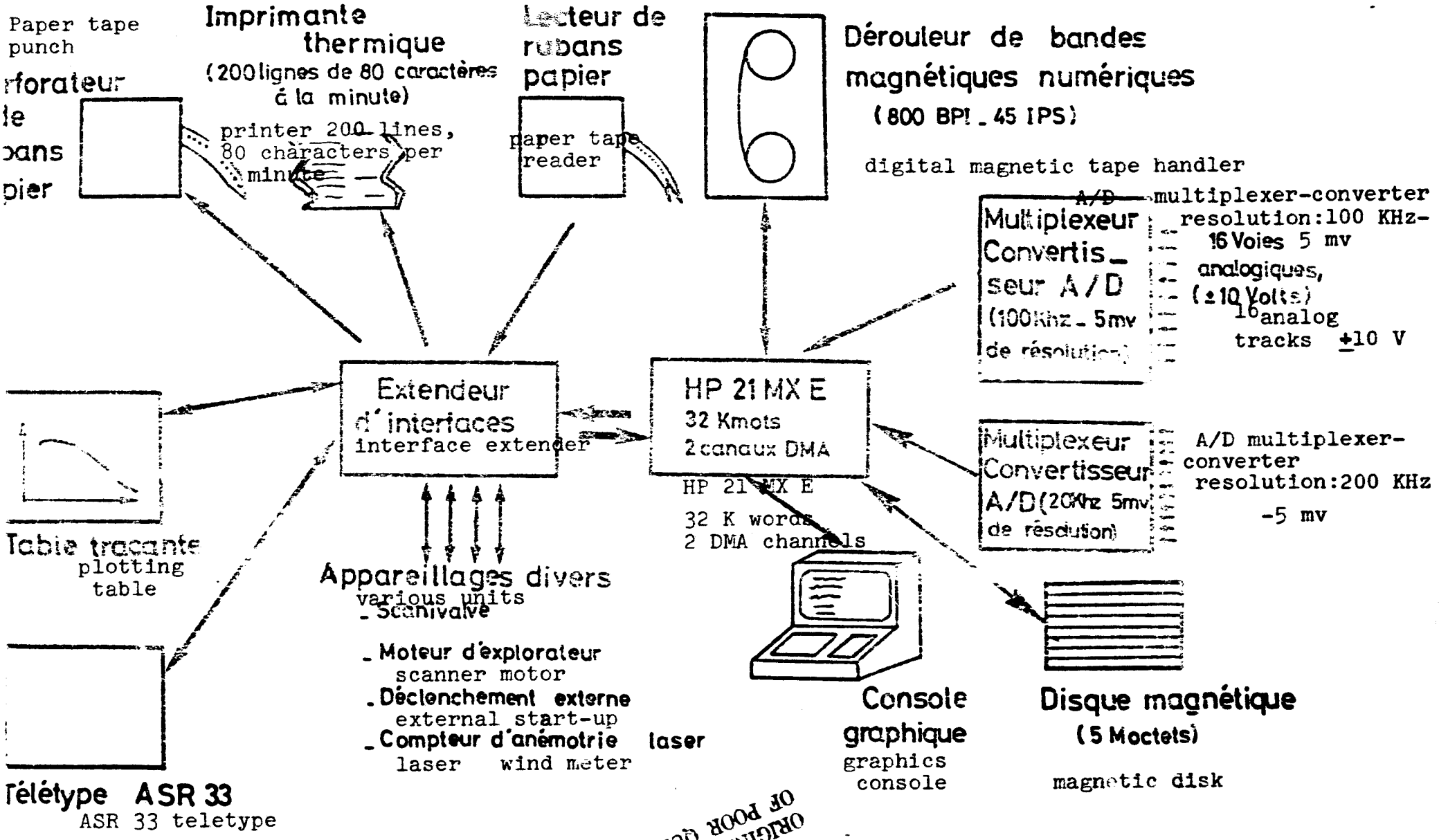

Figure 11: Diagram of the acquisition chain for the T'2 wind tunnel.

Figure 12: Noise from the cold wire at high frequencies (4 kHz).

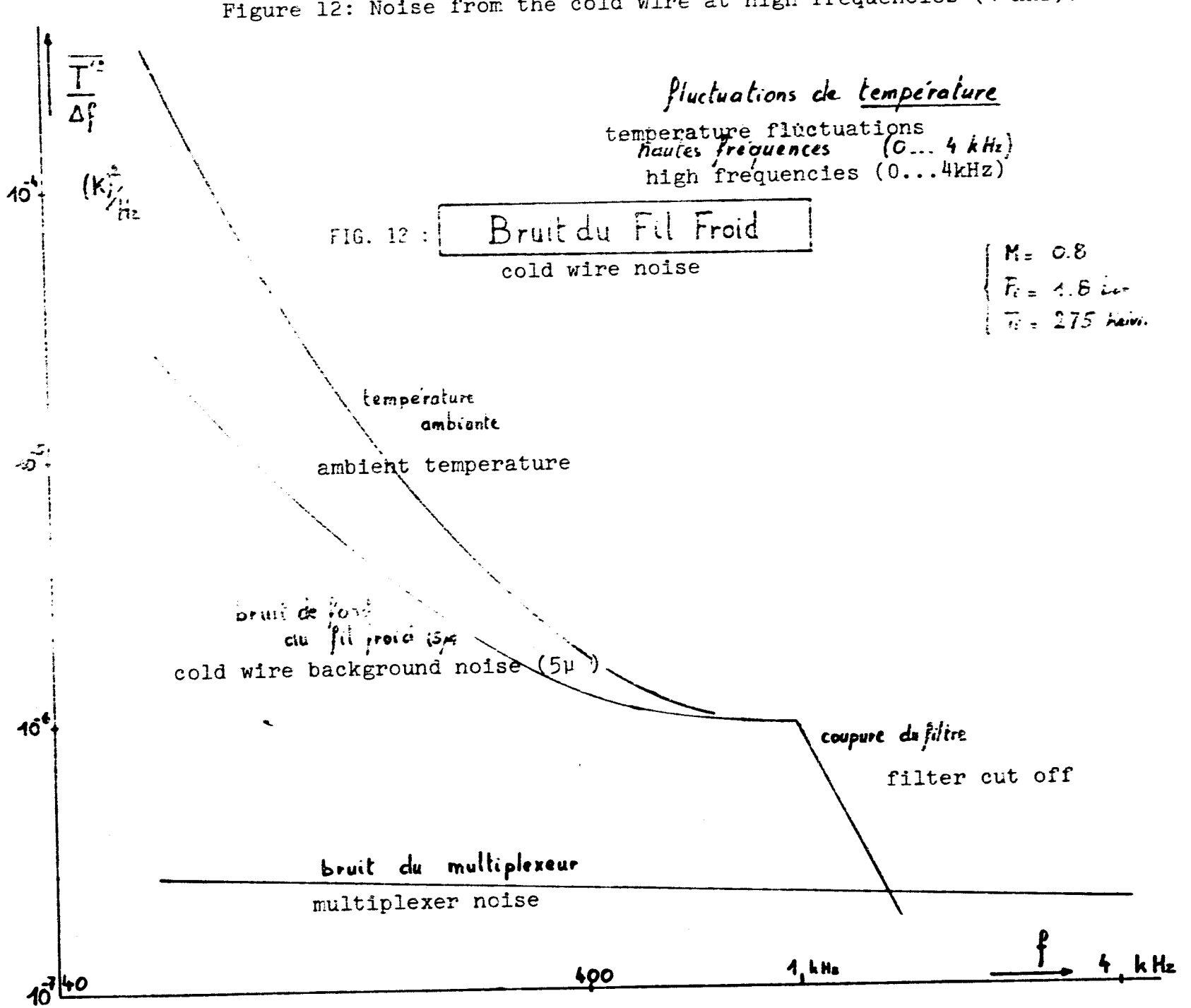

Figure 13: Noise from the cold wire at low frequencies (100 Hz).

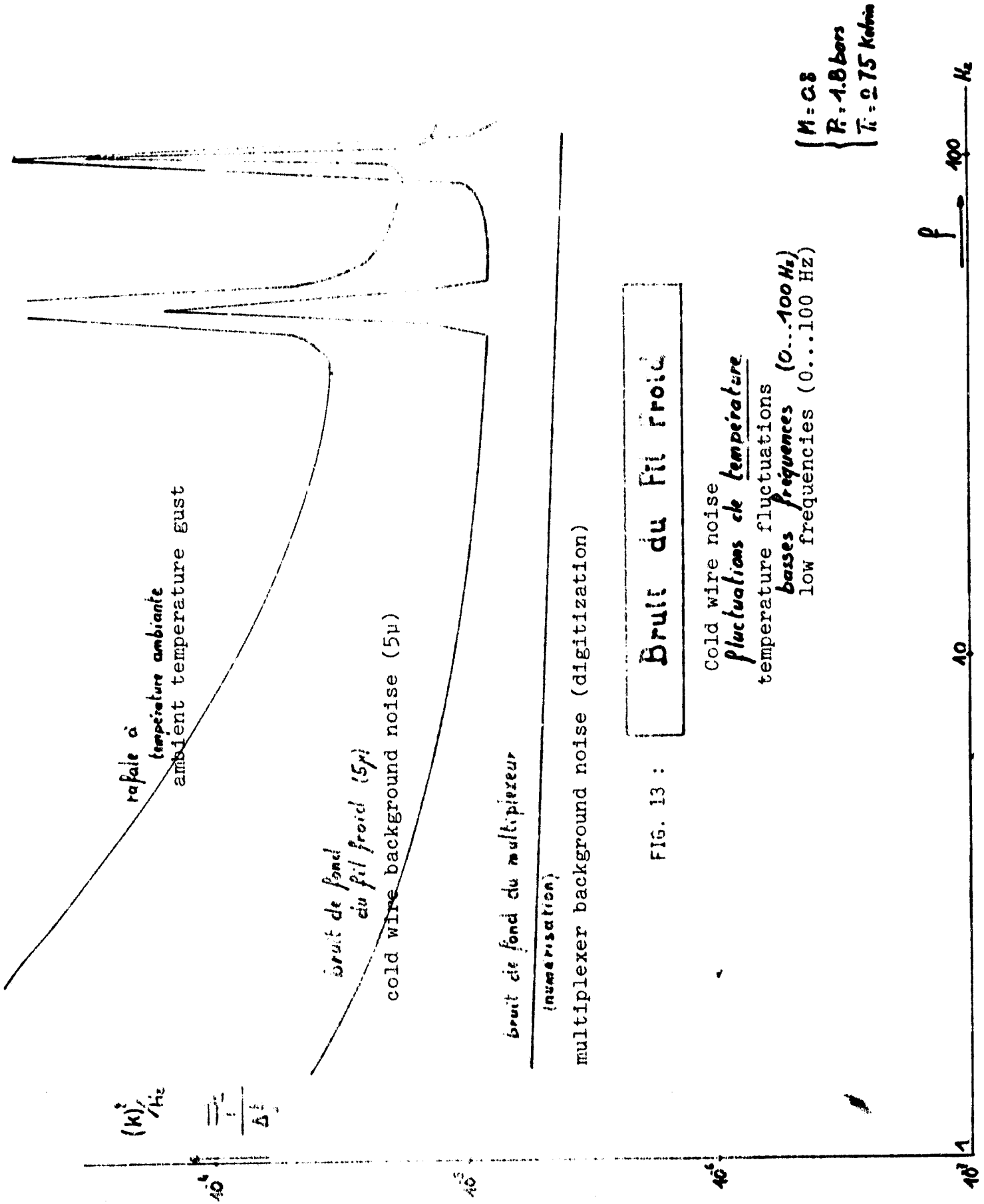

FIG. 13 : **Bruit du Fil froid**

Cold wire noise
Fluctuations de température basses fréquences (0...100 Hz)
temperature fluctuations
low frequencies (0...100 Hz)

Figure 14: Noise from the pressure sensors at high frequencies (4 kHz).

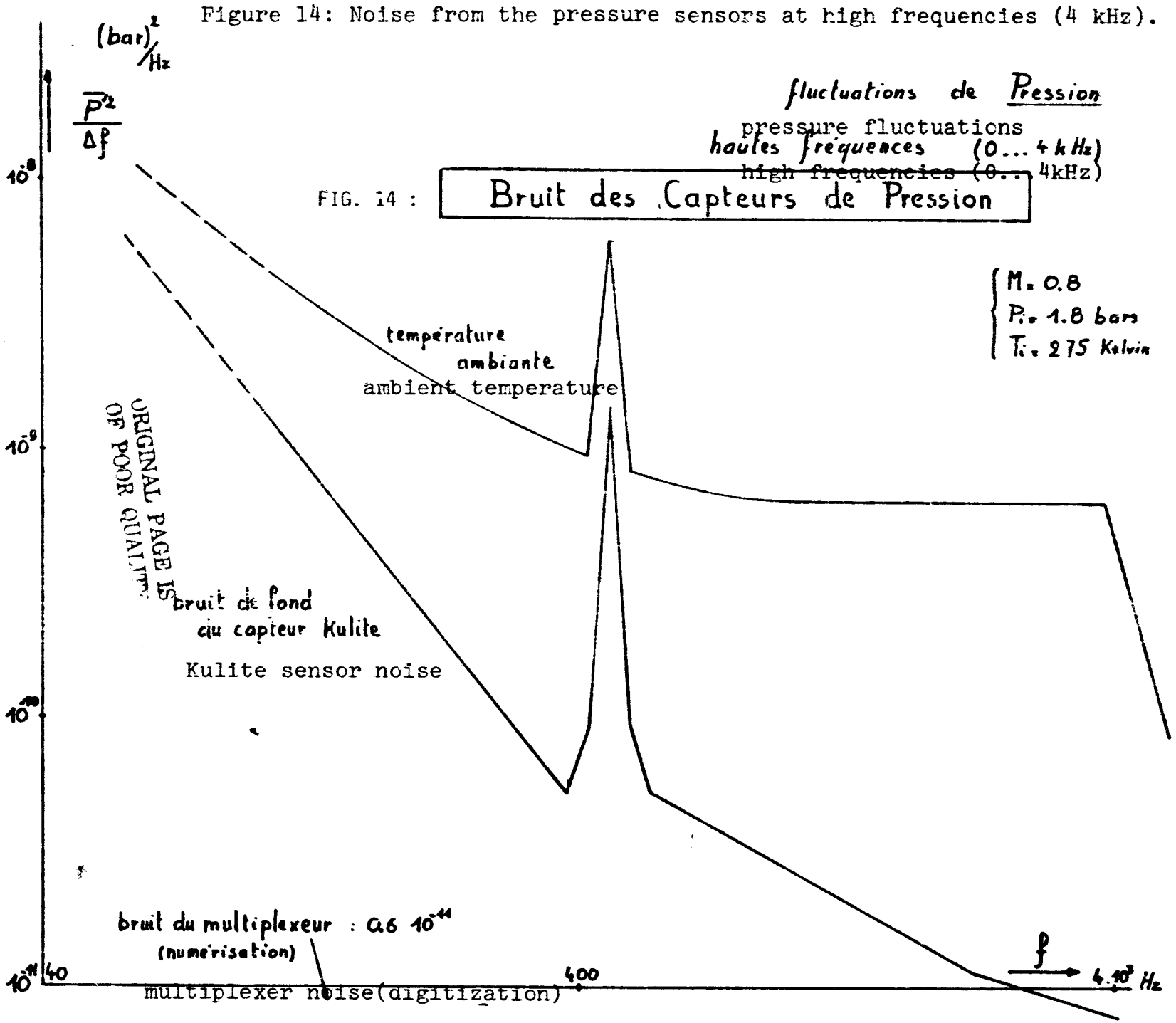

PL. 14

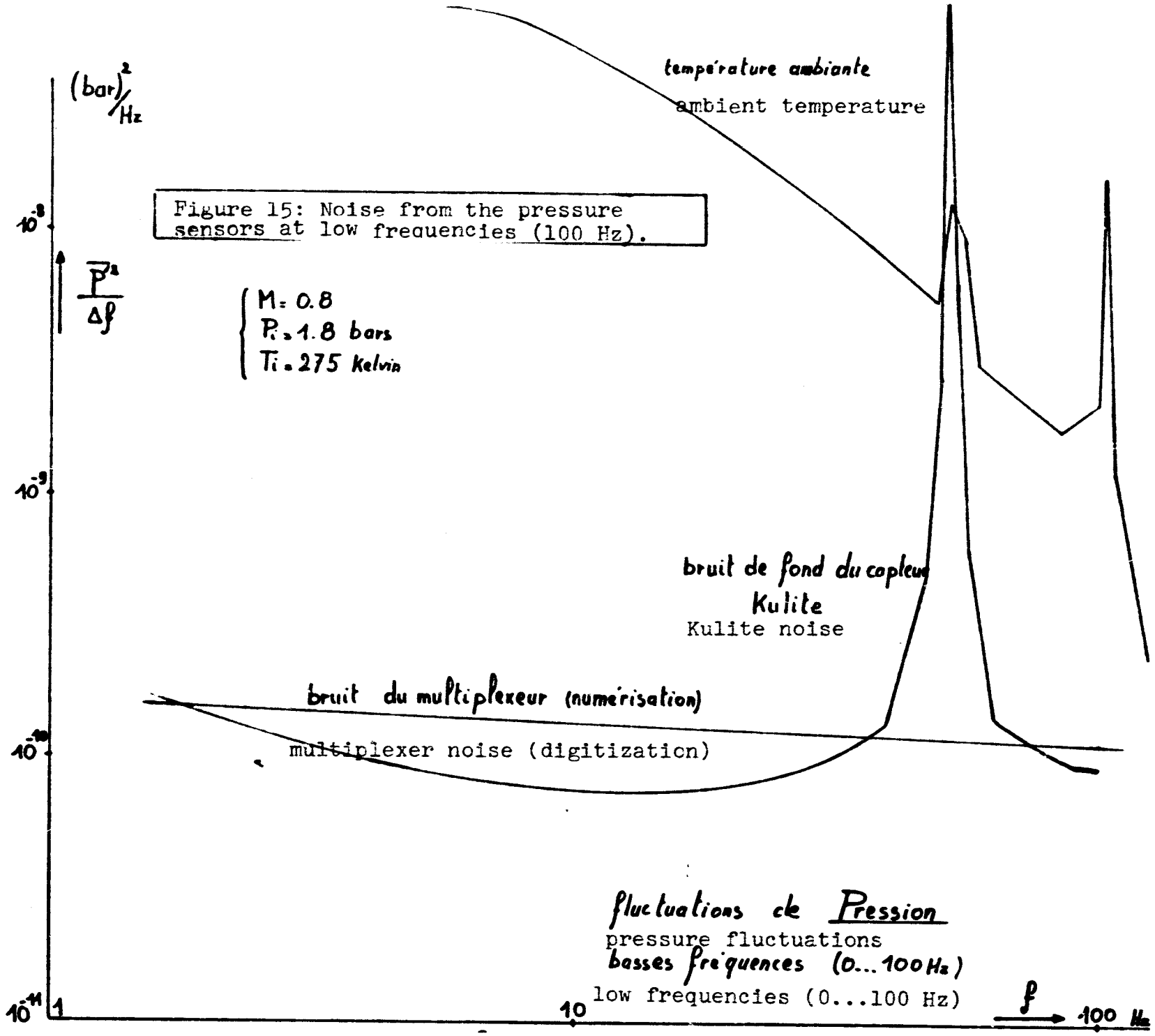

Figure 15: Noise from the pressure sensors at low frequencies (100 Hz).

Pl. 15

Figure 16: Mean level of fluctuation in static pressure measured in the T'2 wind tunnel.

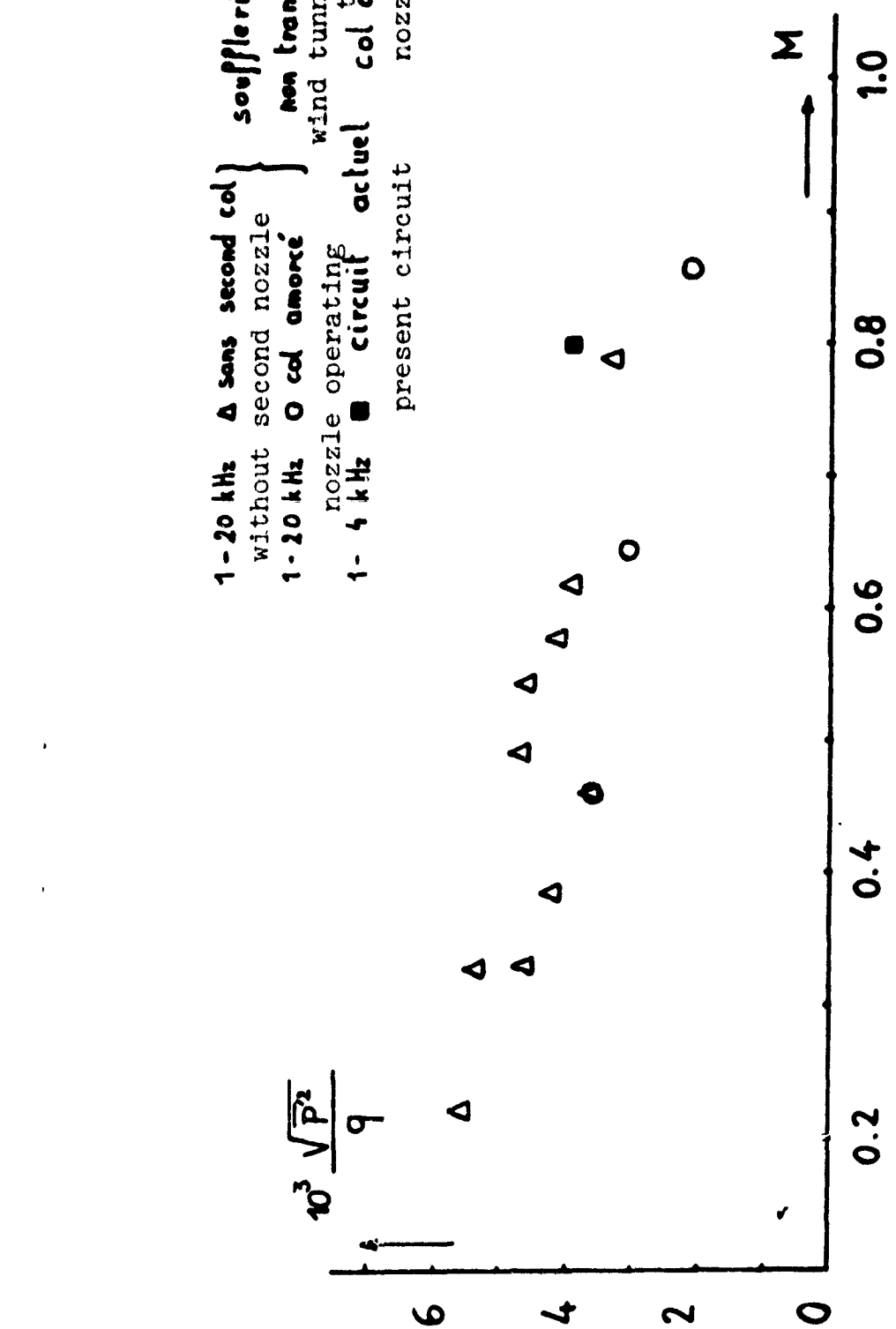

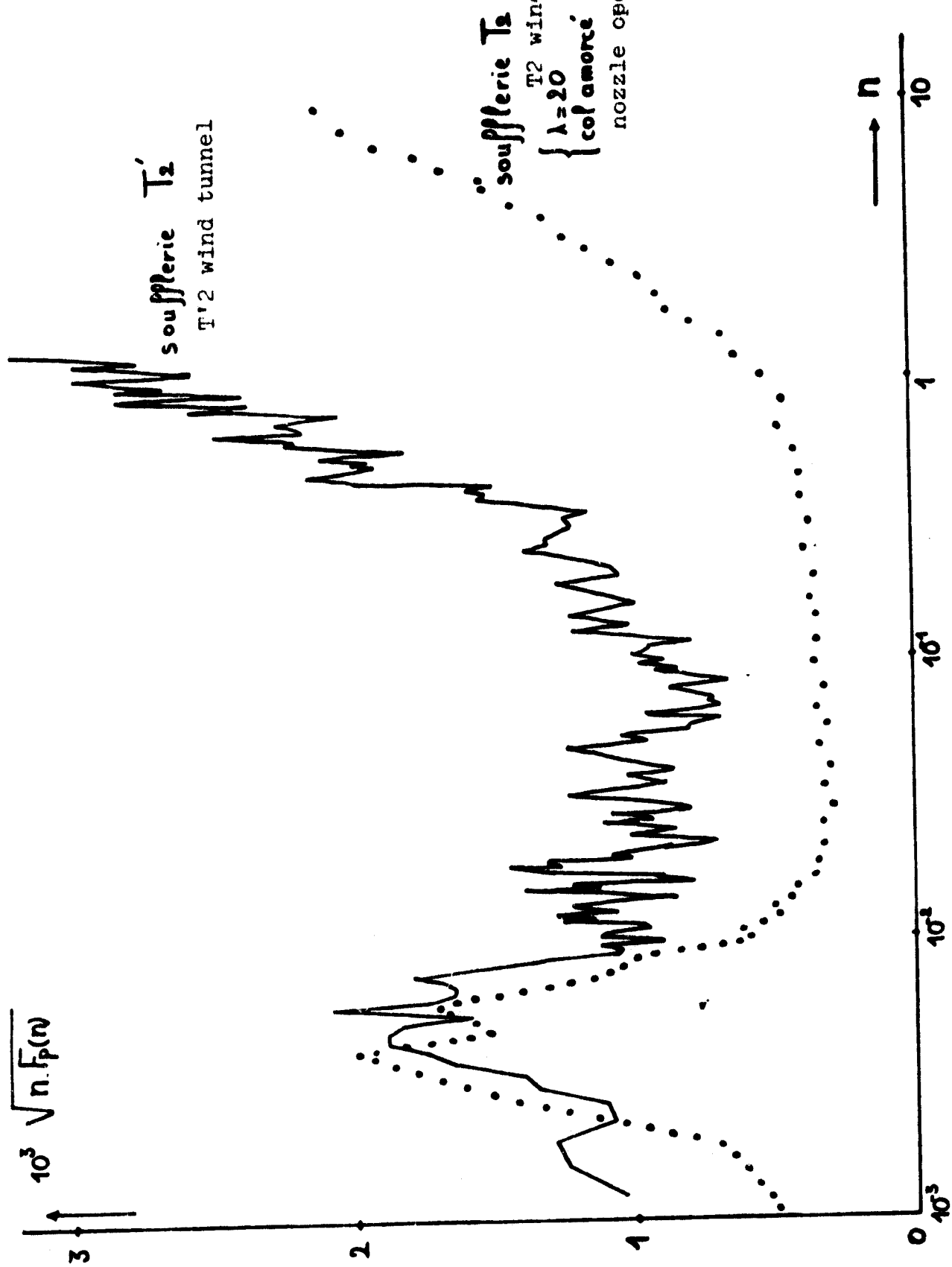

Figure 17: Normalized spectrum of static pressure fluctuations.

Figure 18: Comparison of the spectra taken from the wall and the flow center.

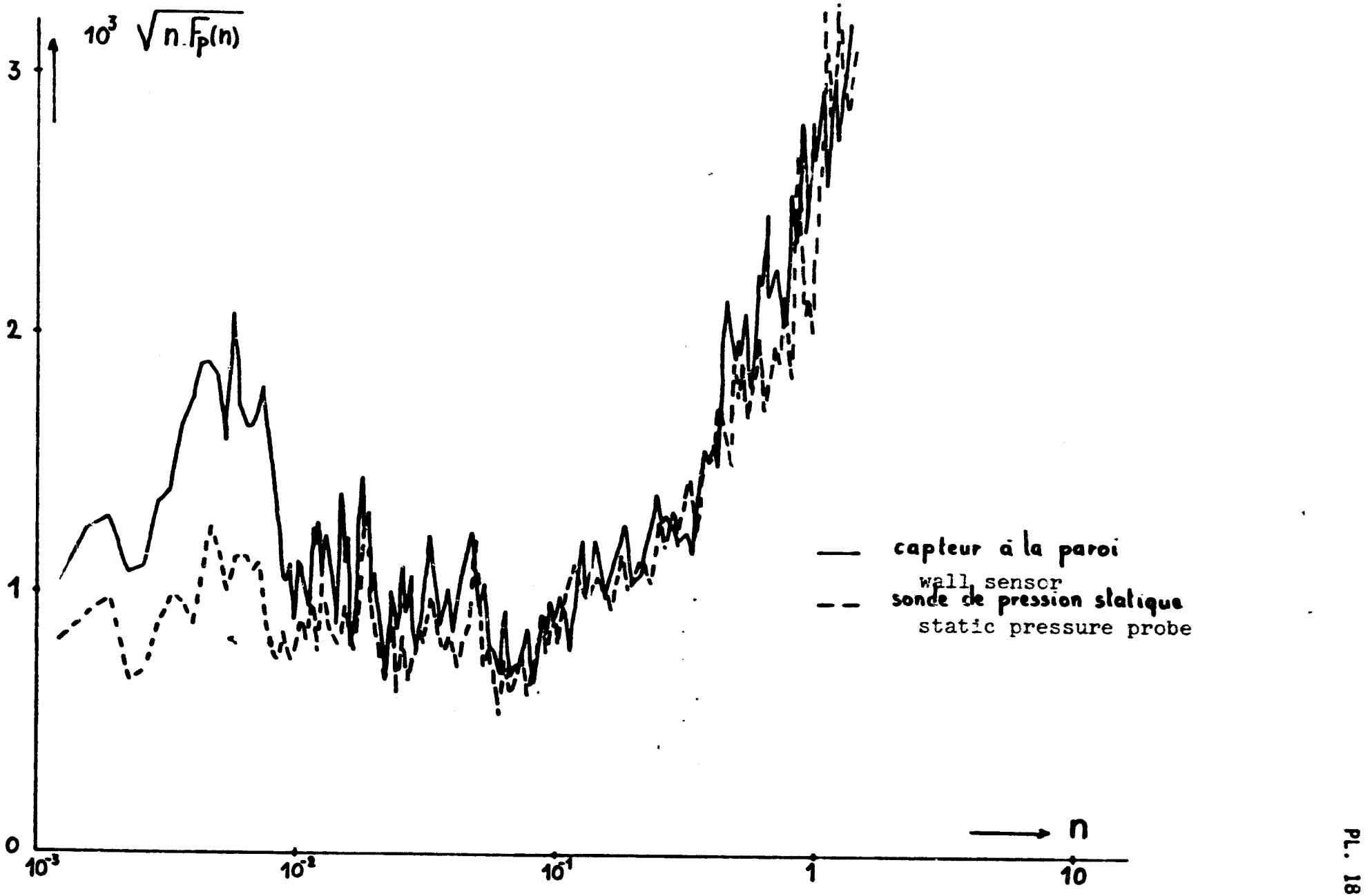

PL. 18

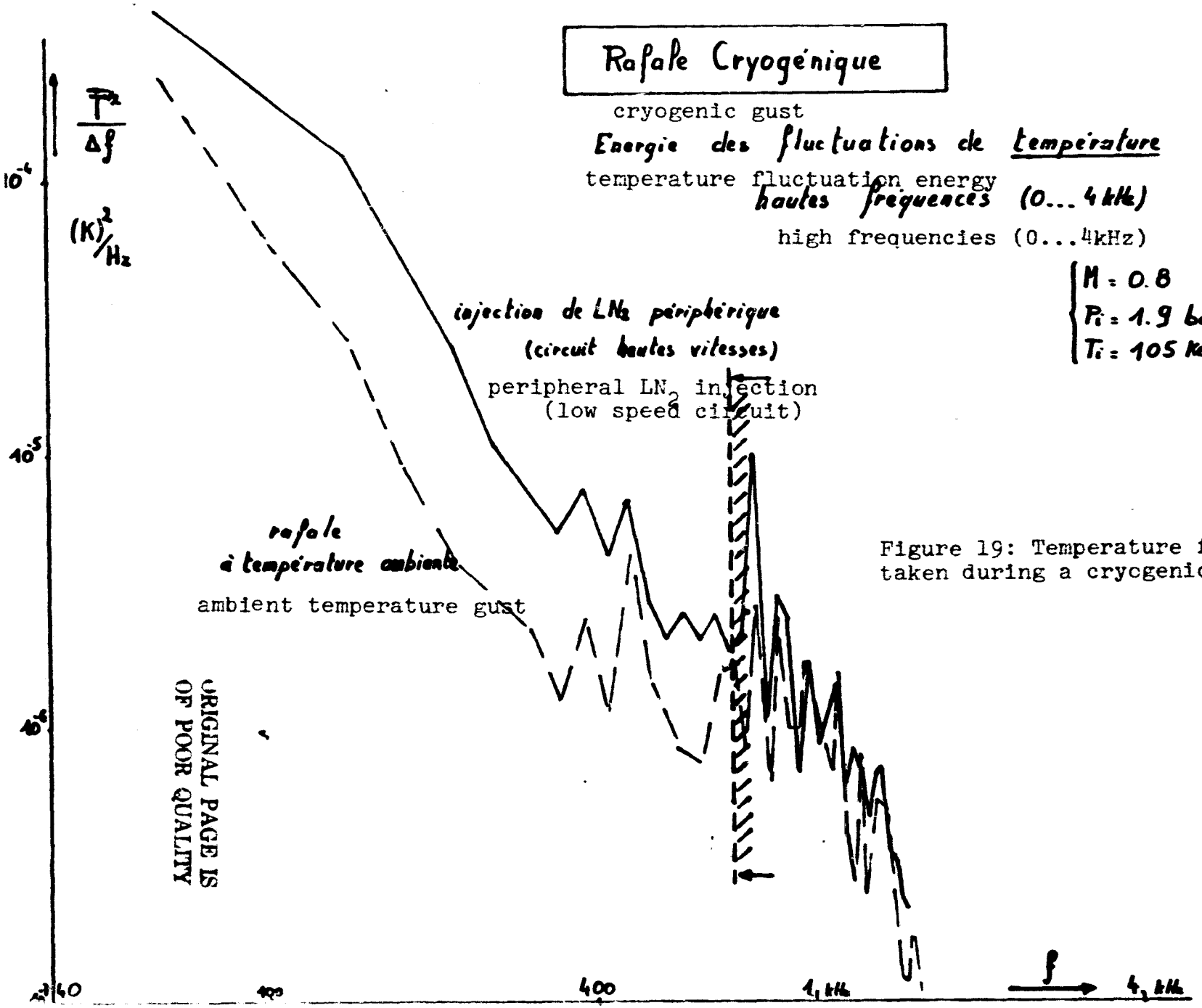

Figure 19: Temperature fluctuation spectrum taken during a cryogenic flow up to 1 kHz.

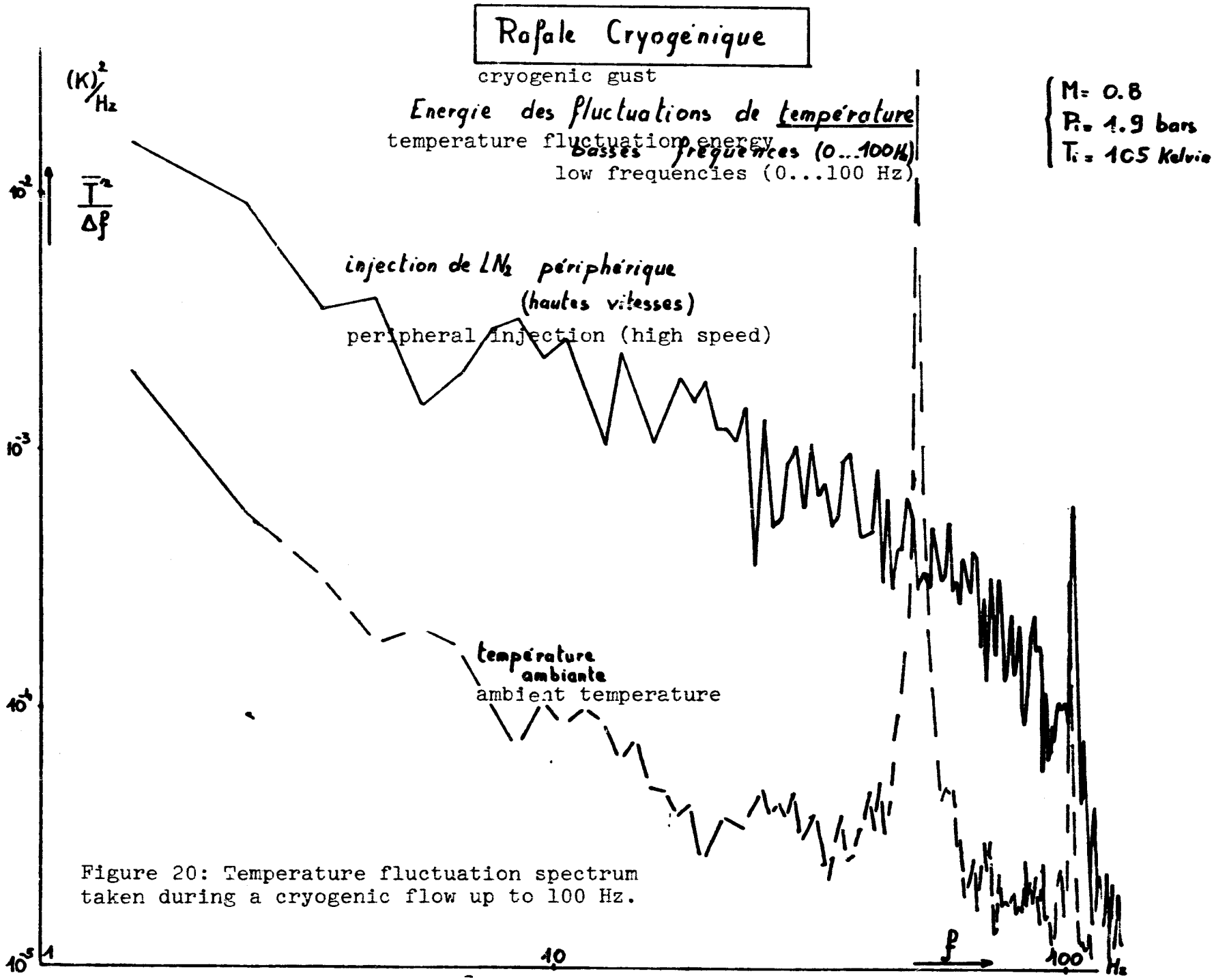

Figure 20: Temperature fluctuation spectrum taken during a cryogenic flow up to 100 Hz.

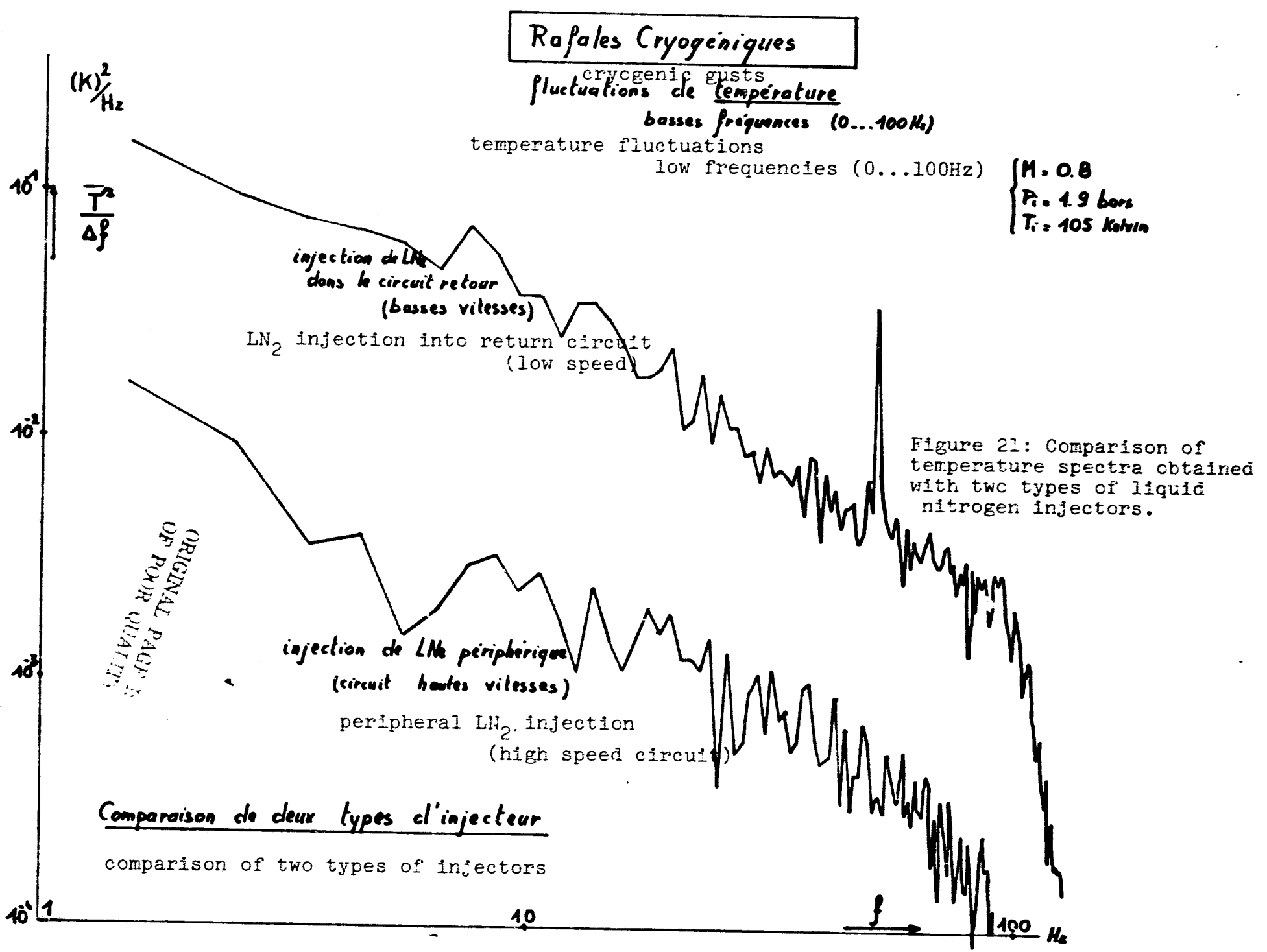

Figure 21: Comparison of temperature spectra obtained with two types of liquid nitrogen injectors.

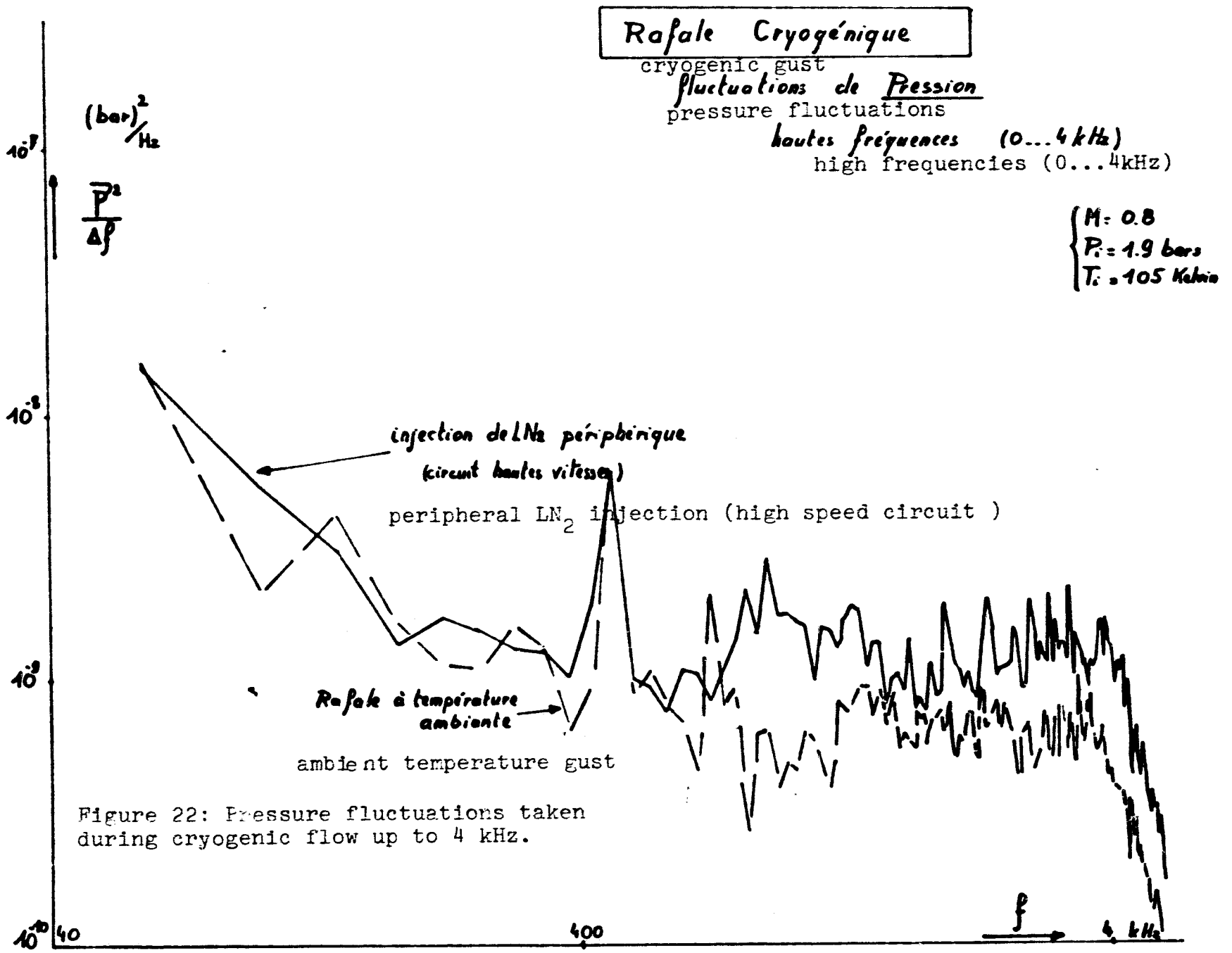

Figure 22: Pressure fluctuations taken during cryogenic flow up to 4 kHz.

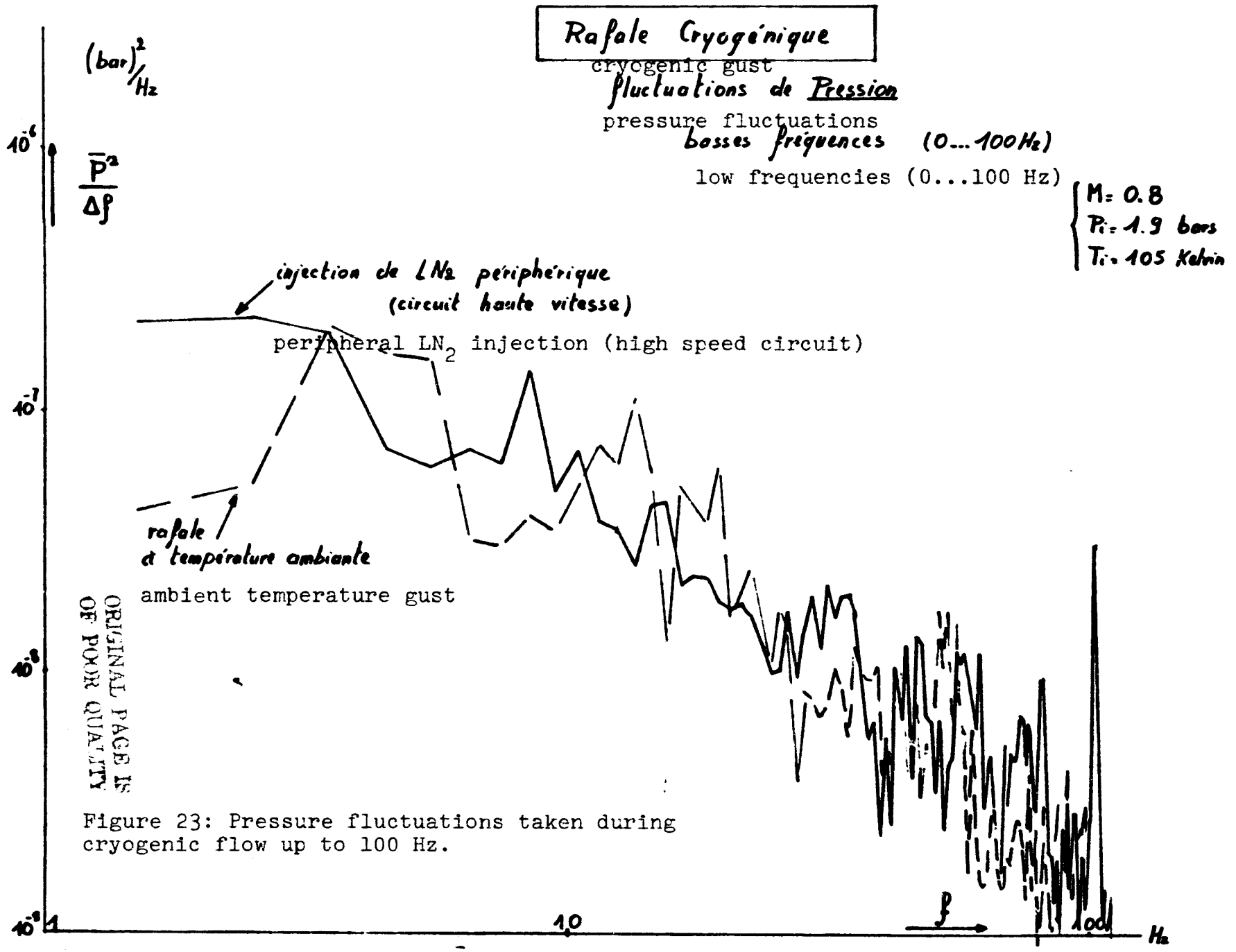

Figure 23: Pressure fluctuations taken during cryogenic flow up to 100 Hz.

Figure 24: Comparison of pressure spectra obtained with two types of liquid nitrogen injectors.

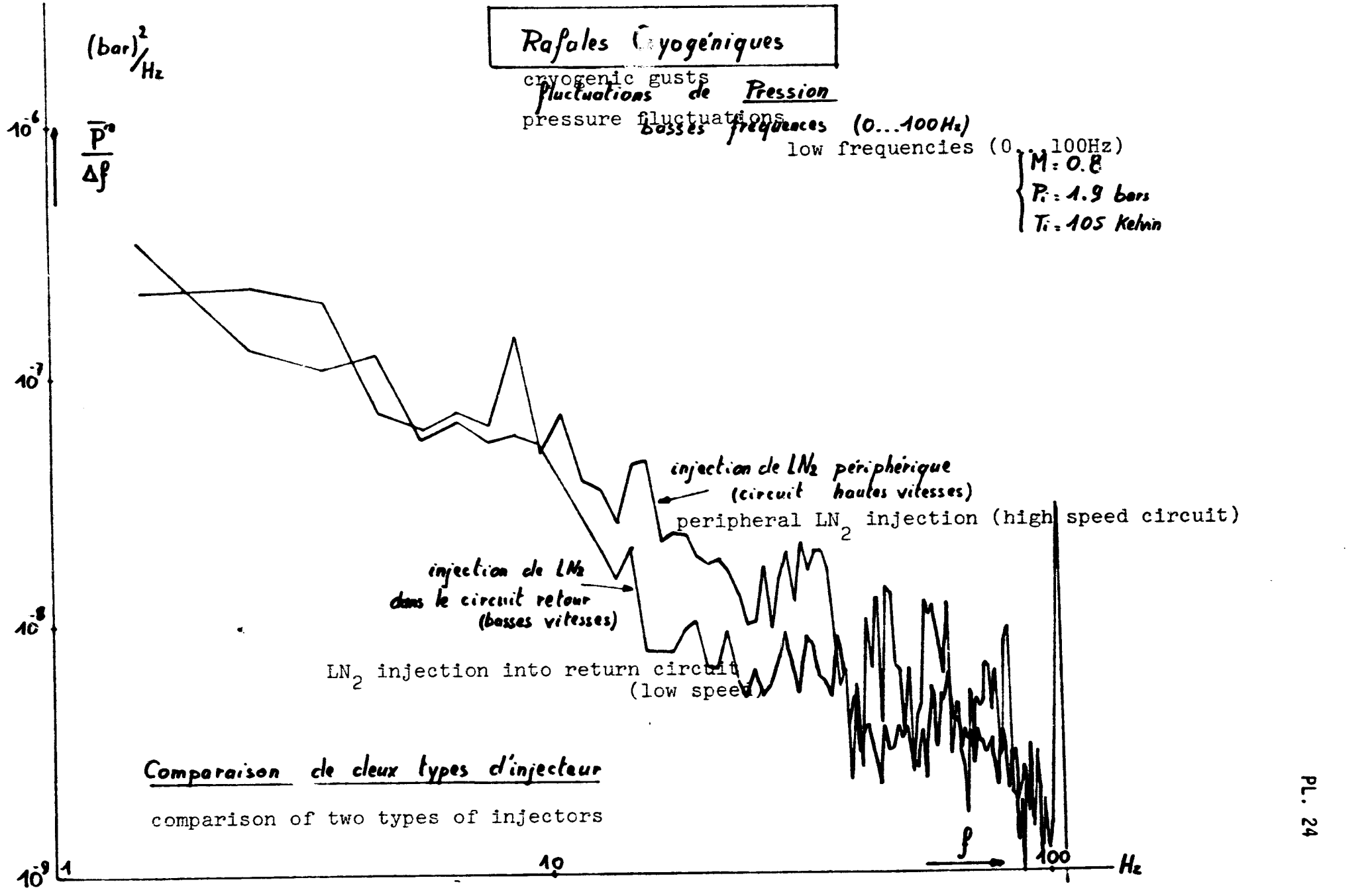

PL. 24

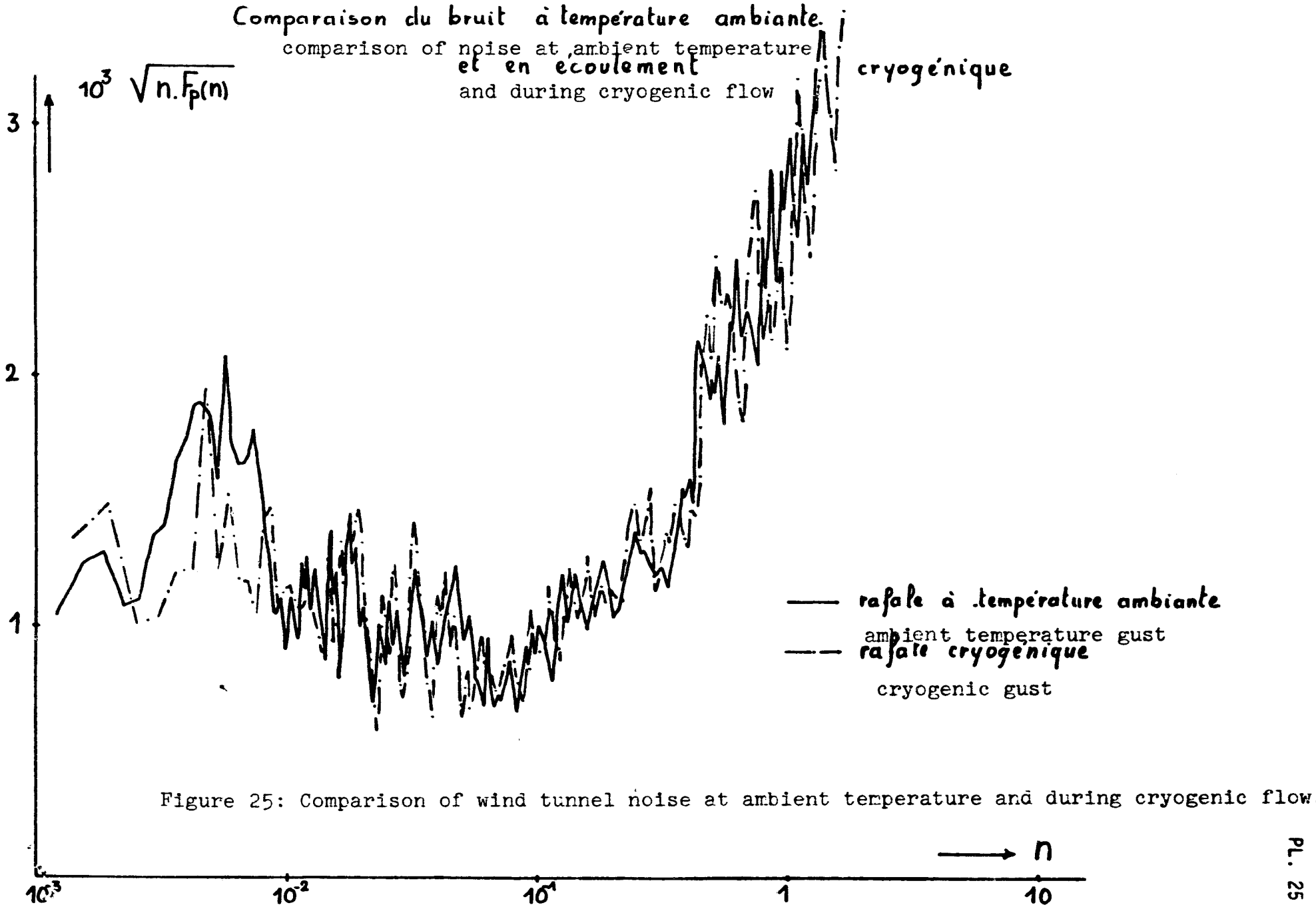

Figure 25: Comparison of wind tunnel noise at ambient temperature and during cryogenic flow.